

PAC-Private Responses with Adversarial Composition

Xiaochen Zhu

MIT

Cambridge, MA, USA

xczhu@mit.edu

Mayuri Sridhar

MIT

Cambridge, MA, USA

mayuri@mit.edu

Srinivas Devadas

MIT

Cambridge, MA, USA

devadas@mit.edu

Abstract

Modern machine learning models are increasingly deployed behind APIs. This renders standard weight-privatization methods (e.g. DP-SGD) unnecessarily noisy at the cost of utility. While model weights may vary significantly across training datasets, model *responses* to specific inputs are much lower dimensional and more stable. This motivates enforcing privacy guarantees directly on model outputs.

We approach this under PAC privacy, which provides instance-based privacy guarantees for arbitrary black-box functions by controlling mutual information (MI). Importantly, PAC privacy explicitly rewards output stability with reduced noise levels. However, a central challenge remains: response privacy requires composing a large number of adaptively chosen, potentially adversarial queries issued by untrusted users, where existing composition results on PAC privacy are inadequate. We introduce a new algorithm that achieves adversarial composition via adaptive noise calibration and prove that mutual information guarantees accumulate linearly under adaptive and adversarial querying.

Experiments across tabular, vision, and NLP tasks show that our method achieves high utility at extremely small per-query privacy budgets. On CIFAR-10, we achieve 87.79% accuracy with a per-step MI budget of 2^{-32} . This enables serving one million queries while provably bounding membership inference attack (MIA) success rates to 51.08% – the same guarantee of $(0.04, 10^{-5})$ -DP. Furthermore, we show that private responses can be used to label public data to distill a publishable privacy-preserving model; using an ImageNet subset as a public dataset, our model distilled from 210,000 responses achieves 91.86% accuracy on CIFAR-10 with MIA success upper-bounded by 50.49%, which is comparable to $(0.02, 10^{-5})$ -DP.

Keywords

PAC privacy, machine learning privacy, adversarial composition, adaptive composition, membership inference attacks

1 Introduction

Machine learning (ML) is increasingly deployed across industries for a wide range of applications. This widespread adoption, however, has raised significant privacy concerns, as models are often trained on sensitive personal information, such as medical records, financial transactions, and private communications [29, 31, 34]. Studies have demonstrated that ML models, particularly over-parameterized neural networks, inadvertently memorize information about their training datasets; this information can be leaked, most notably through membership inference attacks (MIAs), where an adversary infers whether a specific individual’s data was used to train the model [4, 35].



This work is licensed under a Creative Commons Attribution 4.0 International License.

Differential privacy (DP) [13, 15] has emerged as the de facto standard to address these concerns. In ML, this is typically implemented via private training algorithms like DP-SGD [1, 37]. By injecting noise to model gradients during training, this approach yields private model weights that can be safely published under DP guarantees. However, despite its theoretical effectiveness, DP-trained models often face a harsh privacy-utility tradeoff. Achieving acceptable model performance often necessitates a large privacy budget, which weakens the security guarantee [9, 19, 20].

In practice, however, full model weights are rarely published. Instead, modern models are increasingly deployed as black-box services behind remote APIs, where users interact with the system solely via queries and responses [17]. This reality motivates our shift in focus: we propose to directly privatize *model responses* rather than weights. This approach offers three key advantages. First, the response space is typically much lower-dimensional than the parameter space. For instance, image classifiers trained on ImageNet may have millions of parameters, but they only produce confidence scores over 1,000 classes [22]. This significantly reduces the scale of noise required for privacy. Secondly, model responses are far more *stable* than model weights. Small variations in training data can cause substantial changes in the learned weights, but often with minimal differences in their outputs [3, 6]. Finally, privatizing model responses offers black-box compatibility across model architectures, without requiring access to the training dynamics such as gradients.

Applying DP to model responses remains challenging. DP mechanisms calibrate noise to the *sensitivity* of the function, i.e., the maximum change in output over adjacent datasets. In general, tight calculation of sensitivity is NP-hard [48]. While strong stability assumptions can be established for simple or convex learners to bound sensitivity [14], bounding the prediction shift caused by a single training record is generally infeasible for complex non-convex models. Consequently, mechanisms are forced to be pessimistic, assuming sensitivity as high as the full diameter of the output space. This results in excessive noise that fails to exploit the inherent stability of model responses.

Probably approximately correct (PAC) privacy [44, 45] offers a compelling alternative to enable *response privacy*. As an *instance-dependent* framework, PAC privacy is able to measure the underlying stability of an arbitrary data processing function via *black-box simulations*. As a result, PAC privacy rewards stability automatically: functions with stable outputs under the input distribution require significantly less noise to privatize. However, enforcing PAC privacy on a sequence of responses still presents a fundamental theoretical challenge: **adversarial composition**. Unlike the non-adaptive settings, untrusted users can act as adaptive adversaries, selecting queries based on the interaction history to maximize information leakage. Standard composition theorems [44] fail under such adaptivity, while existing adversarial composition [43] performs poorly:

either accumulating privacy leakage *quadratically* in the number of releases, or reverting to DP-like input-independent excessive noise at the cost of utility, as we demonstrate in Section 3.2.

Our Contributions. To address this gap, we introduce a general framework for *posterior-aware adversarial composition*. Our core insight is that, to maintain tight privacy accounting against an adaptive adversary, the curator itself must *adapt* to the adversary’s evolving knowledge. We propose an algorithm with *adaptive noise calibration*, where the curator maintains a belief state representing the posterior distribution of the secret given the interaction history. The curator dynamically calibrates the noise based on this posterior distribution. Under this algorithm, we prove a new adversarial composition theorem that achieves a *linear* accumulation of mutual information. This result overcomes the limitations of prior work, preserving the instance-based utility advantages of PAC privacy with linear composition under adaptive adversarial strategies.

This theoretical result enables the first application of PAC privacy to modern ML models. In particular, we release PAC-private ML responses for model-agnostic classification tasks, while provably limiting MIA success on the sensitive training data. Extensive empirical results across tabular, vision and NLP tasks demonstrate that our method achieves competitive accuracy while supporting millions of queries under tight privacy guarantees. For example, on CIFAR-10, our method achieves an average test accuracy of 87.79% while provably limiting MIA success rate under 51.08% after one million queries, which is the same guarantee provided by $(0.04, 10^{-5})$ -DP. Further, to bridge the gap between finite privacy budgets and the need for unlimited inference, we propose a private model distillation protocol; that is, we use the private responses to label a public auxiliary dataset and train a student model. To mitigate the label noise introduced by privatization, we develop a confidence filtering protocol based on hypothesis testing that provably bounds the probability of retaining mislabeled data. This enables the release of a distilled model that achieves high utility while inheriting the rigorous privacy guarantees of the PAC-private responses. As a proof of concept, we run distillation with auxiliary access to CINIC-10 [7], achieving 91.86% accuracy on CIFAR-10 under a strong PAC privacy guarantee comparable to $(0.02, 10^{-5})$ -DP.

Paper Organization. The remainder of this paper is organized as follows. Section 2 provides the necessary background on the PAC privacy framework. Section 3 presents our main theoretical contribution: the posterior-aware composition framework and the derivation of the linear adversarial composition theorem. In Section 4, we instantiate this framework to release PAC-private ML responses, detailing the threat model, mechanism design, and efficient implementation. Section 5 describes our private model distillation protocol with confidence filtering. Section 6 presents our extensive empirical evaluation across multiple modalities. Section 7 conducts a comprehensive literature review on related work, including differential privacy, and Section 8 concludes the paper.

2 Background

2.1 PAC Privacy

PAC privacy [38, 43–47] is a recently proposed framework that provides instance-specific privacy guarantees. It leverages entropy

in private data, and allows automatic measurement and control of privacy leakage for arbitrary processing functions in a black-box manner. Formally, it is defined as follows:

Definition 2.1 ((δ, ρ, P_S)-PAC Privacy [44]). Let \mathcal{S} be the domain of the sensitive input. Given a possibly randomized function $M : \mathcal{S} \rightarrow \mathcal{R}$, probability distribution P_S over \mathcal{S} , and a binary-valued attack success criterion $\rho : \mathcal{S} \times \mathcal{S} \rightarrow \{0, 1\}$, we say that M satisfies (δ, ρ, P_S) -PAC privacy if for any informed adversary $A : \mathcal{R} \rightarrow \mathcal{S}$, who knows (P_S, M) , takes $R = M(S) \in \mathcal{R}$ as input, and outputs an estimate \hat{S} of S , its success rate measured by the attack criterion ρ , denoted by $1 - \delta_A$, is at most $1 - \delta$, i.e.,

$$1 - \delta_A := \Pr_{S \sim P_S, R \leftarrow M(S), \hat{S} \leftarrow A(R)} [\rho(\hat{S}, S) = 1] \leq 1 - \delta, \quad (1)$$

where the probability is taken over the randomness of S , M , and A .

Remark 2.2. Definition 2.1 guarantees that the adversary cannot win the following security game with probability more than $1 - \delta$: “The data curator draws data $S \sim P_S$ and sends $R = M(S)$ to the adversary. The adversary, knows P_S, M , but not the secret S , returns an estimate \hat{S} . The adversary wins if $\rho(\hat{S}, S) = 1$.” This guarantee is defined under a strong adversary who knows P_S and M and is computationally unbounded. The same bound naturally extends to a realistic adversary who does not know P_S . In machine learning, P_S is typically the distribution from which the training dataset is drawn, and $M(S)$ is the model trained on S or its responses.

While Definition 2.1 bounds the absolute probability of the adversary’s success, it is often easier to quantify and control the *improvement* in the adversary’s performance relative to their prior knowledge. We define this improvement as *posterior advantage*.

Definition 2.3 (Posterior Advantage [44]). For any adversary A as defined in Definition 2.1 who has success rate $(1 - \delta_A)$ under the attack criterion ρ , its *posterior advantage* under f -divergence is

$$\Delta_f \delta_A := D_f(\text{Bern}(\delta_A) \parallel \text{Bern}(\delta_0)) = \delta_0 f\left(\frac{\delta_A}{\delta_0}\right) + (1 - \delta_0) f\left(\frac{1 - \delta_A}{1 - \delta_0}\right)$$

where D_f is some f -divergence and $1 - \delta_0$ is the *optimal prior success rate* for an *a priori* adversary who only knows P_S and M without observing $M(S)$, i.e., $1 - \delta_0 := \max_Q \Pr_{S \sim P_S, \hat{S} \sim Q} [\rho(\hat{S}, S) = 1]$.

Given the distribution P_S and attack criterion ρ , the optimal prior success rate $(1 - \delta_0)$ is a known constant. For example, in membership inference attacks where P_S is specified such that each data point is included in the training set with 50% probability, the optimal prior success rate is exactly 50%. Since the prior is fixed, we can limit the adversary’s final success rate $(1 - \delta_A)$ simply by controlling their posterior advantage $\Delta_f \delta_A$. The foundation of PAC privacy lies in the connection between an arbitrary adversary’s posterior advantage and the mutual information (MI) between the input and the output, as established in the following theorem.

THEOREM 2.4 ([44]). *For any adversary A , its posterior advantage satisfies $\Delta_f \delta_A \leq \inf_{P_W} D_f(P_{S, M(S)} \parallel P_S \otimes P_W)$, where P_W is the distribution of an arbitrary random variable W with support \mathcal{R} . In particular, when D_f is the KL-divergence and $P_W = P_{M(S)}$, we have*

$$\Delta_{\text{KL}} \delta_A = (1 - \delta_A) \log \frac{1 - \delta_A}{1 - \delta_0} + \delta_A \log \frac{\delta_A}{\delta_0} \leq I(S; M(S)), \quad (2)$$

where $I(\cdot; \cdot)$ is the mutual information between two random variables.

We note that this upper bound is *attack-agnostic*: the mutual information $I(S; M(S))$ depends only on P_S and M , and bounds the advantage for *any* attack criterion ρ . Hence, one can privatize an algorithm against arbitrary adversaries simply by setting a mutual information budget B and enforcing $I(S; M(S)) \leq B$. Then, concrete guarantees on adversarial success rate can be derived via Eq. (2).

For deterministic functions $M : \mathcal{S} \rightarrow \mathbb{R}^d$, the following theorem determines the required scale of Gaussian noise such that the noisy mechanism satisfies such a MI budget, and hence, is PAC-private.

THEOREM 2.5 (NOISE DETERMINATION [38, 44]). *Given random variable $S \sim P_S$, a deterministic function $M : \mathcal{S} \rightarrow \mathbb{R}^d$ and a mutual information budget $B > 0$, let $\text{Var}(M(S)) = U\Lambda U^\top$ be the singular value decomposition (SVD) of the covariance matrix of $M(S)$, where $\Lambda = \text{diag}(\lambda_1, \dots, \lambda_d)$. Define diagonal matrix Λ_B as*

$$\Lambda_B = \text{diag} \left(\frac{\sqrt{\lambda_i} \sum_{j=1}^d \sqrt{\lambda_j}}{2B} : i = 1, \dots, d \right).$$

Then, $I(S; M(S) + Z) \leq B$ where $S \sim P_S$ and $Z \sim \mathcal{N}(0, U\Lambda_B U^\top)$.

Remark 2.6. Theorem 2.5 controls the MI by adding Gaussian noise given the covariance matrix of the output $M(S)$. This matrix may be evaluated in its exact form, for example, when the secret space \mathcal{S} is tractable with size $m := |\mathcal{S}|$; indeed, for the instantiation considered in this paper, exact evaluation is feasible. The major computational cost under this case is to evaluate $M(S)$ for all $S \in \mathcal{S}$. Once the m outputs are collected, we optimize noise calibration by performing SVD directly on the weighted, centered $m \times d$ matrix in $O(md \cdot \min(m, d))$ time, avoiding explicit covariance formation. This decomposition also enables efficient noise sampling via linear transformation in $O(d^2)$ time. Consequently, the total complexity to calibrate and sample the noise is $O(mC + md \cdot \min(m, d) + d^2)$, where C is the cost of a single evaluation of the function M . The total complexity is typically dominated by the evaluation term mC .

When \mathcal{S} is computationally intractable, one can *estimate* the covariance matrix by Monte Carlo simulation, i.e., sampling S from P_S and evaluating $M(S)$ for $m' \ll m$ times in a black-box manner. Xiao and Devadas [44] determine the sampling complexity m' as a function of the budget B and a confidence parameter γ , to ensure that the estimated covariance is sufficiently precise. Alternatively, Sridhar et al. [38] propose the empirical convergence of variance estimation as a practical criterion for sufficient sampling.

In both cases, the m or m' samples for noise calibration are independent of the underlying realized secret S . Operationally, the data curator samples a secret $S \sim P_S$, calibrates the noise covariance matrix Σ based on P_S , M , and B , and releases $M(S) + \mathcal{N}(0, \Sigma)$.

2.2 Membership Inference Attacks

Membership inference attacks (MIAs) have become the de facto standard to empirically measure privacy leakage in ML. To provide a concrete understanding of the PAC privacy guarantees, we translate the MI budget B into a guarantee on the MIA success rate. We formalize MIA to match the PAC privacy framework as follows:

Definition 2.7 (Membership Inference Attack [38]). *Given a finite data pool $U = \{u_1, \dots, u_n\}$ and a processing mechanism M , let $S \sim P_S$ be a subset of U randomly selected according to distribution P_S . An informed adversary A , knowing (U, P_S, M) and observing $M(S)$,*

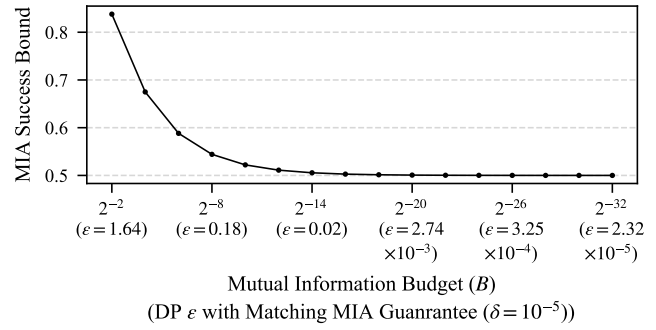


Figure 1: Provable upper bound on the individual MIA success rate as a function of the MI budget B , under a uniform prior success rate of 50%. Differential privacy parameters with matching guarantees are showed in brackets for reference.

outputs a membership estimate $\hat{S} \subseteq U$. The *individual membership inference success rate* for a user u_i is defined as the probability that the adversary correctly determines their membership:

$$1 - \delta_{A,i} := \Pr_{S \sim P_S, \hat{S} \leftarrow A(M(S))} [\mathbb{1}\{u_i \in S\} = \mathbb{1}\{u_i \in \hat{S}\}],$$

where $\mathbb{1}\{E\}$ is the indicator variable for event E .

This definition allows us to treat membership inference for any data point u_i as a specific instance of the attack criterion ρ in Definition 2.1. The bound derived in Theorem 2.4 applies directly.

As discussed previously, given the MI budget B , Eq. (2) allows us to numerically solve for the upper bound on the adversary's success rate $(1 - \delta_{A,i})$. In particular, if P_S is specified s.t. $\forall i, \Pr(u_i \in S) = 1/2$, i.e., the prior success rate is $1 - \delta_{0,i} = 50\%$, a budget of $B = 2^{-2}$ provably limits the MIA success rate to 83.78%. Tightening to $B = 2^{-10}$ reduces this bound to 52.21%, and an extremely strict budget of $B = 2^{-32}$ results in a guarantee of $\approx 50.001\%$, virtually indistinguishable from random guessing. These bounds apply simultaneously to every individual data point in U , as the prior success rate is uniform across the population. For context, (ϵ, δ) -DP [15] also theoretically bounds MIA success by $1 - (1 - \delta)/(1 + e^\epsilon)$ [38]: $(1, 10^{-5})$ -DP provably limits MIA success to 73.11%, while $(0.1, 10^{-5})$ -DP reduces it to 52.50%. Fig. 1 illustrates the theoretical upper bounds on MIA success rate across different MI budgets as well as their corresponding DP parameters. While the privacy notions differ semantically, we provide these comparable DP parameters throughout the paper to serve as a familiar reference for our PAC privacy guarantees. We provide a more comprehensive discussion on DP in Section 7.

3 Adversarial Composition

The PAC privacy guarantees introduced in Section 2 apply to mechanisms with a single release. However, if we enforce PAC privacy guarantees on sequential responses, each release involves a standalone mechanism. Understanding how the privacy leakage accumulates (or equivalently, how the privacy guarantee composes) under multiple releases requires rigorous composition analysis.

Standard composition theorems for PAC privacy study non-adaptive settings in which the sequence of mechanisms is fixed in advance or independent of past outputs, and show that the MI guarantee accumulates linearly [44]. However, many practical use

cases are inherently adaptive. For example, in stochastic gradient descent (SGD), each mechanism corresponds to a gradient computation step that depends on the current model parameters, which is a function of all previous gradient outputs. Moreover, in response privacy, the sequence of queries is not only adaptive to previous releases but may also be adversarial, as a user can strategically choose future queries based on observed outputs to maximize information leakage. In these cases, the sequence of mechanisms is neither independent nor pre-defined, but instead depends on the entire interaction history. This adaptivity allows later mechanisms to amplify information revealed by earlier outputs, even when each individual release satisfies a strong per-query PAC privacy guarantee. Therefore, non-adaptive composition theorems cannot be directly applied, and naively composing per-step guarantees can lead to incorrect bounds on the total information leakage.

In this section, we formalize an adversarial composition setting for PAC privacy where each mechanism may be adaptively chosen based on past outputs via a strategy unknown to the data curator. We then present a composition algorithm that calibrates noise *adaptively* to the interaction history and prove that the mutual information guarantee accumulates *linearly* despite adaptivity.

3.1 Setting

Following Section 2, let random variable $S \in \mathcal{S}$ represent the secret input data. Let $t = 1, 2, \dots, T$ be discrete time steps. At initialization ($t = 0$), the data curator samples the secret $S \sim P_S$. At each time step t , an adaptive adversary, who wishes to gain knowledge about S , provides the data curator with a processing function $M_t : \mathcal{S} \rightarrow \mathcal{R}_t$, where $\mathcal{R}_t = \mathbb{R}^{d_t}$. In response, the data curator releases $R_t \in \mathcal{R}_t$, a possibly noisy version of $M_t(S)$. We define random variable $\mathcal{T}_t = \{(M_i, R_i)\}_{i=1}^t$ as the full *transcript* of the interaction history up to time step t . The transcript comprises both the adversary's chosen mechanisms and the data curator's releases, with $\mathcal{T}_0 = \emptyset$.

In particular, the adversary may be *adaptive*, whose choices are defined by a sequence of unknown strategies $\{F_t\}_{t=1}^T$. At time step t , the adversary observes the transcript \mathcal{T}_{t-1} and samples the next query $M_t \sim F_t(\mathcal{T}_{t-1})$, where $M_t : \mathcal{S} \rightarrow \mathbb{R}^{d_t}$. Given a transcript \mathcal{T}_{t-1} , the adversarial strategy F_t defines a distribution over all possible functions from \mathcal{S} to \mathbb{R}^{d_t} and is unknown to the data curator.

The only assumption we make about the adversary is that they have no side-channel access to the secret. While a strong, informed adversary knows the distribution P_S of the secret, they can only gain knowledge about the realized S by interacting with the curator and observing their responses. In particular, the choice of the next query function M_t depends on S only via the transcript \mathcal{T}_{t-1} . Formally,

$$M_t \perp S \mid \mathcal{T}_{t-1}. \quad (3)$$

We emphasize that the data curator uses the *identical* secret input S when evaluating M_t at each step. This persistence is essential for meaningful privacy analysis. Recall the previous MIA example where P_S defines a distribution over subsets of U s.t. $\forall u \in U P(u \in S) = 1/2$. In the context of ML, MIA adversaries are interested in knowing if a particular example $u \in U$ is *ever* used across all the responses. If the curator re-samples at each step, the probability that an arbitrary u is included in *at least one* sampled subset rapidly approaches 1 as T increases. A prior success rate near 100% renders any bound on the posterior advantage vacuous. By fixing S , we

ensure that the input distribution of the overall mechanism remains P_S , and hence the prior MIA success rate remains constant, i.e., 50%. Thus, any privacy loss is strictly due to leakage from responses, rather than increased prior success rates. While this setting is crucial for meaningful privacy guarantees, it presents a greater challenge to bound the overall leakage compared to independent re-sampling: the adversary can aggregate information from the entire transcript \mathcal{T}_T to refine their knowledge about the single, persistent secret S .

3.2 Posterior-Aware Composition

Our goal is to bound the total mutual information leakage of the overall mechanism accumulated over T steps, i.e., $I(S; R_1, \dots, R_T)$. By Theorem 2.4, this then bounds the posterior advantage and consequently, the adversarial success probability. By the chain rule of MI, the overall MI decomposes into the sum of conditional MIs:

$$I(S; R_1, \dots, R_T) = \sum_{t=1}^T I(S; R_t \mid R_1, \dots, R_{t-1}).$$

Hence, a natural approach is to bound each term by a per-step mutual information budget b_t . However, this is not trivial.

One straightforward attempt is to apply Theorem 2.5 at every step t to calibrate noise scale Σ_t for the mechanism M_t such that $I(S; R_t) \leq b_t$ where $R_t = M_t(S) + \mathcal{N}(0, \Sigma_t)$. However, this is not sufficient as it fails to account for the dependencies between releases. For instance, in a simple case of privatizing two adaptively chosen mechanisms, the total mutual information is $I(S; R_1, R_2) = I(S; R_1) + I(S; R_2 \mid R_1)$; however, Theorem 2.5 only enforces that $I(S; R_1) \leq b_1$ and $I(S; R_2) \leq b_2$ independently for $S \sim P_S$. Even if the marginal leakage $I(S; R_2)$ is small, the conditional leakage $I(S; R_2 \mid R_1)$ remains unbounded because the adversary may choose M_2 adaptively to exploit the information revealed by R_1 .

One theoretical workaround [43] is to enforce a stronger worst-case bound for each release, i.e., calibrate noise scale Σ_t to bound $\sup_Q I_{S \sim Q}(S; M_t(S) + \mathcal{N}(0, \Sigma_t)) \leq b'_t$ and $I(S; M_t(S) + \mathcal{N}(0, \Sigma_t)) \leq b_t$ simultaneously for each t . The former constraint directly bounds the conditional MI given any possible transcript, effectively enforcing an *input-independent, worst-case guarantee*, similar to that of local differential privacy [12]. However, as detailed in Appendix A, this forces a harsh trade-off: one must either accept a composition bound that scales quadratically in T , or add excessive noise for a DP-like input-independent guarantee that ignores the instance-specific stability. This negates the core benefits of PAC privacy.

Fundamentally, the issue of this static composition approach comes from *noise misspecification*. From the perspective of an informed adversary, its belief on the distribution of S changes over time. Before any observations, an informed adversary knows S is sampled from P_S as its prior belief, which is usually the uniform distribution over \mathcal{S} . After observing the history \mathcal{T}_{t-1} , any rational adversary would be tracking the posterior distribution $P_{S \mid \mathcal{T}_{t-1}}$ based on the observed transcript to refine their knowledge of the secret. In the aforementioned approach, the data curator calibrates noise based on P_S at all steps. Hence, the mechanism only protects against an adversary who has observed nothing, rather than one who has already learned from the interactions. To provide a tight guarantee on the conditional leakage $I(S; R_t \mid \mathcal{T}_{t-1})$, the noise must

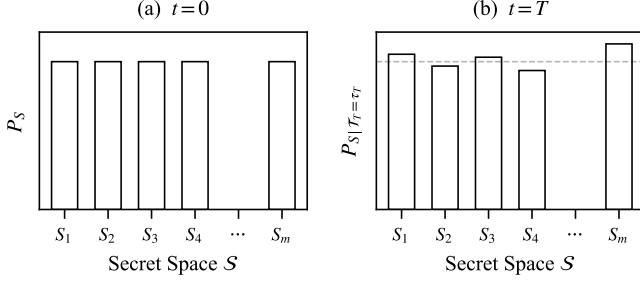


Figure 2: An informed adversary refines their knowledge of the secret by tracking the posterior distribution of the secret conditioned on the observed transcript. In response, the curator adaptively calibrates noise to bound the conditional MI given the current transcript, i.e., the expected KL divergence between the posterior distribution and the prior P_S .

be calibrated *adaptively* with respect to the *current* posterior, effectively responding to the adversary's knowledge. Equivalently, bounding the conditional MI bounds the expected KL divergence between the adversary's posterior belief on the distribution of S and the prior P_S , limiting the adversary's capabilities to refine their knowledge of the secret. This is illustrated in Fig. 2.

To formalize this, we first define a helper function that determines the Gaussian noise required to bound the leakage of a specific processing function *under a specific input distribution*. This extends the noise determination mechanism from Theorem 2.5 by treating the noise scale as a function of the input distribution as well.

Definition 3.1 (Noise Calibration Function Σ). A function $\Sigma : \mathcal{P}(\mathcal{S}) \times (\mathbb{R}^d)^{\mathcal{S}} \times \mathbb{R}_{>0} \rightarrow \mathbb{R}^{d \times d}$ is said to be a noise calibration function if the following bound holds for any distribution P over \mathcal{S} , deterministic function $M : \mathcal{S} \rightarrow \mathbb{R}^d$, and positive real number B :

$$I_{S \sim P}(S; M(S) + \mathcal{N}(0, \Sigma(P, M, B)) \leq B.$$

We can instantiate such a function Σ using Theorem 2.5.

Equipped with this definition, we present an algorithm that allows the curator to achieve *posterior-aware composition* via Bayesian posterior updates in Algorithm 1. The mechanism explicitly maintains a belief state P_t , which represents the posterior distribution of the secret S given the current history \mathcal{T}_t . At $t = 0$, the curator samples the secret $S \sim P_S$ and initializes the belief state, identical to the prior distribution $P_0 = P_S$. At each step, the adversary chooses a query M_t , via its querying strategy F_t that is unknown to the curator. Upon receiving M_t , the curator calculates the noise covariance $\Sigma_t = \Sigma(P_{t-1}, M_t, b_t)$ required to satisfy the privacy budget for query function M_t under the *current belief* P_{t-1} . Sampling the additive noise from $\mathcal{N}(0, \Sigma_t)$, the curator releases the noisy response $M_t(S) + \mathcal{N}(0, \Sigma_t)$, and then updates the belief using Bayes' rule: $\forall s \in \mathcal{S}$,

$$P_t(s) \propto \exp\left(-\frac{1}{2} (R_t - M_t(s))^T \Sigma_t^{-1} (R_t - M_t(s))\right) \cdot P_{t-1}(s). \quad (4)$$

We now analyze the privacy guarantee and computational complexity of Algorithm 1.

Algorithm 1 Posterior-Aware Composition

```

1: Input: Prior  $P_S$ , per-step mutual information budgets  $\{b_t\}_{t=1}^T$ , noise calibration function  $\Sigma$ , horizon  $T$ . The adversary additionally holds strategies  $\{F_t\}_{t=1}^T$  unknown to the curator.
2: Initialize:
3:   Initial belief  $P_0 \leftarrow P_S$ 
4:   Transcript  $\mathcal{T}_0 \leftarrow \emptyset$ 
5:   Sample secret  $S \sim P_S$ 
6: for  $t = 1, 2, \dots, T$  do:
7:   Adversary step:
8:     Adversary samples  $M_t : \mathcal{S} \rightarrow \mathbb{R}^{d_t}$  from  $F_t(\mathcal{T}_{t-1})$ 
9:   Adaptive noise calibration:
10:     $\Sigma_t \leftarrow \Sigma(P_{t-1}, M_t, b_t)$ 
11:   Release:
12:    Release  $R_t \leftarrow M_t(S) + \mathcal{N}(0, \Sigma_t)$ 
13:   Update:
14:    Update history  $\mathcal{T}_t \leftarrow (\mathcal{T}_{t-1}, (M_t, R_t))$ 
15:    Update posterior belief conditioned on  $\mathcal{T}_t$ :  $\forall s \in \mathcal{S}$ ,
16:     $P_t(s) \propto \exp(-\frac{1}{2} (R_t - M_t(s))^T \Sigma_t^{-1} (R_t - M_t(s))) \cdot P_{t-1}(s)$ 
17: end for

```

3.2.1 Privacy Guarantee. We show that under Algorithm 1, the per-step MI bounds compose linearly to bound the overall MI. This matches the non-adaptive setting [44] despite adversarial adaptivity. First, we prove that the belief state P_t maintained by the algorithm via Eq. (4) correctly tracks the true posterior of S , which is the same distribution maintained by an informed and optimal adversary.

LEMMA 3.2 (VALIDITY OF POSTERIOR UPDATE). *Let \mathcal{T}_t be the random variable representing the transcript up to time t generated by Algorithm 1. For any time step $0 \leq t \leq T$ and any transcript τ_t realizable at t , when conditioned on $\mathcal{T}_t = \tau_t$, the belief state P_t maintained by the curator is the same as the posterior distribution of the secret maintained by an informed and optimal adversary: $P_t = P_{S|\mathcal{T}_t=\tau_t}$.*

PROOF. This is a Bayesian inference step and we can prove the statement via induction. Full proof is deferred to Appendix B.1. \square

We proceed to prove the main composition theorem. As the noise is calibrated adaptively to the true posterior, we can bound the conditional MI at each step exactly by b_t , allowing linear composition.

THEOREM 3.3 (ADVERSARIAL COMPOSITION). *Fix a prior P_S over the secret space \mathcal{S} and a horizon $T \in \mathbb{N}$. Let (R_1, \dots, R_T) be the sequence of releases produced by Algorithm 1 run with step MI budgets $\{b_t\}_{t=1}^T$, against an arbitrary adaptive adversary $(F_t)_{t=1}^T$.*

Then, the mutual information between the secret input S and the full sequence of T releases (R_1, \dots, R_T) satisfies

$$I(S; R_1, \dots, R_T) \leq B_T := \sum_{t=1}^T b_t.$$

PROOF. We prove a stronger statement that $I(S; R_1, \dots, R_T) \leq I(S; \mathcal{T}_T) \leq B_T$. Full proof is deferred to Appendix B.2. \square

Remark 3.4. Theorem 3.3 also bounds the expected KL divergence between the adversary's posterior belief of the secret's distribution and the prior distribution P_S : $\mathbb{E}_{\mathcal{T}_T} [D_{\text{KL}}(P_{S|\mathcal{T}_T=\tau_T} \parallel P_S)] =$

Table 1: The PAC privacy guarantees on MIA success rate under a 50% prior success rate after $1 \leq T \leq 10^6$ responses across different levels of per-step MI budget b . The table also includes the maximum number of responses such that the guarantee matches that of $\epsilon \leq 1$ and 8 under DP ($\delta = 10^{-5}$).

b	2^{-4}	2^{-8}	2^{-12}	2^{-16}	2^{-20}	2^{-24}	2^{-28}	2^{-32}
$T = 1$	67.5	54.4	51.1	50.3	50.07	50.02	50.00	50.00
$T = 10$	98.7	63.9	53.5	50.9	50.22	50.05	50.01	50.00
$T = 10^2$	100	91.0	61.0	52.8	50.69	50.17	50.04	50.01
$T = 10^3$	100	100	83.4	58.7	52.18	50.55	50.14	50.03
$T = 10^4$	100	100	100	76.9	56.89	51.73	50.43	50.11
$T = 10^5$	100	100	100	100	71.48	55.45	51.36	50.34
$T = 10^6$	100	100	100	100	100	67.09	54.31	51.08
T s.t. $\epsilon \leq 1$	1	28	454	7K	116K	2M	30M	477M
T s.t. $\epsilon \leq 8$	11	176	3K	45K	724K	12M	185M	3B

$I(S; \mathcal{T}_T) \leq B_T$. Intuitively, this limits the adversary’s power to refine its knowledge on S and perform inference attacks on S (cf. Fig. 2).

Theorem 3.3 shows that when the noise calibration is adaptive to the interaction transcript, the per-step mutual information budgets $\{b_t\}$ compose linearly to a total bound of $B_T = \sum_{t=1}^T b_t$. Consequently, under a uniform budget allocation where $b_t = b$ for all t , the total MI after T releases is upper bounded by $B_T = bT$.

To illustrate the practical implications, we return to the MIA example under a uniform 50% prior success rate (cf. Section 2.2). Recall from Section 3.1 that the secret S is sampled once and persistent across responses, hence, the adversary’s prior success rate remains constant at 50% regardless of T . Table 1 presents the theoretical upper bound on a MIA adversary’s success rate under varying budgets b and horizons T . Table 1 also lists the maximum number of queries the system can take before the guarantee reaches the equivalent of $\epsilon = 1$ or 8 under DP. Under a per-step budget of $b = 2^{-8}$, MIA success is bounded by 54.42% after a single response (matching the guarantee of DP with $\epsilon \approx 0.18$), rising to 91% ($\epsilon \approx 2.31$) after 100 responses. With a much tighter budget of $b = 2^{-32}$, the privacy loss is almost negligible: even after *one million responses*, MIA success is still bounded by 51.08%, matching $\epsilon \approx 0.04$ under DP. In fact, under this budget, the system can support up to ≈ 477 *million responses* before reaching the same guarantee as $(1, 10^{-5})$ -DP. This capacity exceeds the lifetime query volume of many real-world deployments, effectively rendering the privacy budget inexhaustible.

3.2.2 Computational Complexity. While Algorithm 1 is theoretically valid for any secret space \mathcal{S} , we first analyze its computational complexity under the tractable setting where $m = |\mathcal{S}|$ is finite. As discussed in Remark 2.6, for a single release, noise calibration and sampling requires $O(mC + md \cdot \min(m, d) + d^2)$ time, dominated by the evaluation term $O(mC)$. For applications in this paper, $d < m$, and this cost becomes $O(mC + md^2)$. Algorithm 1 introduces an additional step of posterior update for each release, which reuses the eigen-decomposition obtained during noise calibration. This allows us to avoid explicit matrix inversion in Eq. (4) and compute the likelihoods via efficient vector projections in $O(md^2)$ time. Consequently, the additional belief-tracking step in Algorithm 1 incurs

no additional asymptotic overhead, while being negligible compared to the $O(mC)$ cost for m evaluations.

In cases where $|\mathcal{S}|$ is intractable (e.g., when \mathcal{S} is a continuous space and $|\mathcal{S}|$ is infinite), maintaining the full posterior distribution P_t is not feasible. However, we note that P_t is only used in the noise calibration step where we need to evaluate the covariance matrix of the output distribution $M(S)$ under $S \sim P_{t-1}$. Similar techniques discussed in Remark 2.6 can be employed to *estimate* such covariance under P_{t-1} . As mentioned previously, for applications exhibited in this paper, \mathcal{S} is indeed finite and tractable, and the exact evaluation of P_t is feasible and efficient. We leave a more detailed discussion on the intractable case to future work.

4 PAC-Private Machine Learning Responses

Section 3 introduces an adversarial composition framework that achieves linear composition with the presence of an adaptive adversary. As discussed, this is applicable to a wide range of applications, such as stochastic gradient descent. In this section, we focus on response privacy in ML, and instantiate Algorithm 1 to release PAC-private predictions made by a ML model trained on sensitive data. Fig. 3 illustrates an overview for our proposed system.

4.1 Setting and Threat Model

Consider a supervised learning setting for a classification task with d classes. Let $U = \{(x_i, y_i)\}_{i=1}^n \subset \mathcal{X} \times \mathcal{Y}$ denote the universe of all possible data points, where \mathcal{X} is the input space and $\mathcal{Y} = \{1, \dots, d\}$ is the label space. As discussed in Section 2.2, we employ a *subsampling-based* input distribution to enable provable defense against MIA, following the standard practice in PAC privacy [38, 44]. Specifically, the secret input S is a random subset of U drawn from a prior distribution P_S over \mathcal{S} , a collection of subsets of U . P_S is specified such that for each individual data point $(x, y) \in U$, the probability that (x, y) is included in S is 50%. This establishes a balanced membership inference game with a uniform prior success rate of 50%. The sampled secret input dataset S is then used to train an underlying ML model that generates predictions on user queries. We emphasize that the same secret set S is used for all responses.

4.1.1 Threat Model. We assume a *strong adversary* with unbounded compute. This adversary possesses full knowledge of the universe U , the secret space \mathcal{S} , the prior distribution P_S , and the exact training and inference algorithms used by the curator. However, the adversary does not know the realized secret dataset S .

At each time step $t = 1, 2, \dots$, the adversary submits a query $q_t \in \mathcal{X}$ to the curator. These queries can be chosen adaptively based on the transcript of previous queries and responses, and can also be selected adversarially to maximize information leakage regarding a specific target in the universe U . Upon receiving q_t , the curator performs inference using the model trained on S and returns a response, potentially injecting noise to ensure PAC privacy. The adversary’s goal is to determine whether a target individual $u^* \in U$ is a member of the secret set S with a success rate significantly higher than the prior baseline of 50%.

We note that this threat model assumes a potent adversary with complete knowledge of the system except for the realized secret dataset while being computationally unbounded. In practice, a realistic adversary will have limited computational resources and is

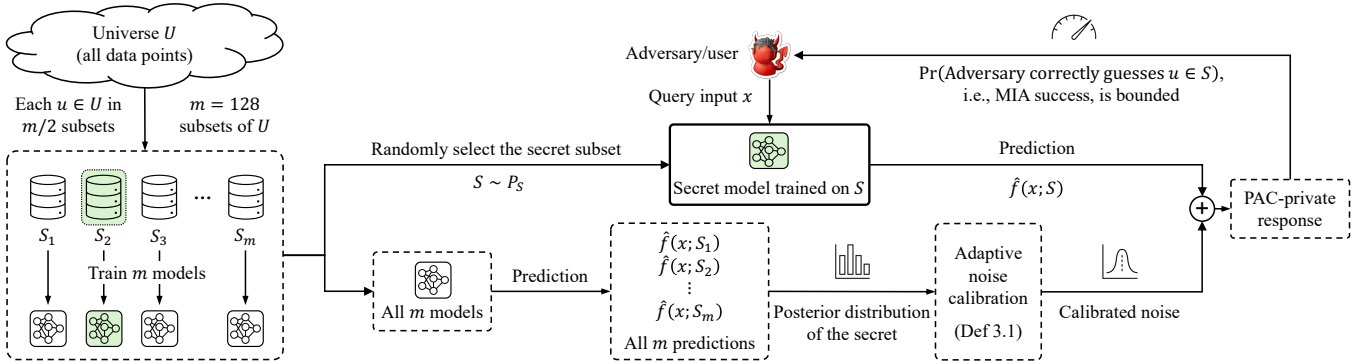


Figure 3: An overview of our proposed system to release PAC-private machine learning responses to an adversary’s queries.

unlikely to know P_S or the training/inference algorithms used by the curator. Nevertheless, security established under the potent adversary model naturally extends to the realistic setting.

4.2 Concrete Instantiation

As established in Section 2, PAC privacy bounds the success of an informed adversary by limiting the mutual information between the secret input S and the released responses. Under adaptive and adversarial mechanism selection, Algorithm 1 ensures the total leakage remains bounded. We now instantiate this algorithm for PAC-private machine learning responses.

4.2.1 Input Distribution. To instantiate Algorithm 1, we must first specify the distribution P_S from which the secret dataset S is sampled. A canonical choice for P_S is the uniform distribution over all 2^n subsets of U , i.e., Poisson subsampling where each point in U is selected independently with probability 0.5. However, the exponential size of this support renders exact noise calibration and posterior belief update computationally intractable. Instead, following prior work [38], we adopt a tractable construction where the support is restricted to a finite collection of m subsets, i.e., $\mathcal{S} = \{S_1, \dots, S_m\}$. The prior P_S is then defined as the uniform distribution over \mathcal{S} . While Sridhar et al. [38] generated \mathcal{S} via random half-partitioning to create $m/2$ pairs of disjoint sets, we introduce a modified construction to better approximate the canonical Poisson setting. In particular, for each $u \in U$, we randomly select $m/2$ indices from $\{1, 2, \dots, m\}$ and assign u to the corresponding subsets. Crucially, this construction ensures that the marginal distribution of $S \sim P_S$ matches Poisson subsampling with $p = 0.5$. The only distinction is that the security game is now played over a reduced support of size m , rather than over the intractable space of all 2^n subsets. This enables efficient and exact execution of Algorithm 1.

Choice of m . Our PAC privacy guarantees on the posterior MIA success rate hold for any even integer $m \geq 2$. However, because we assume a strong adversary who knows the construction of \mathcal{S} and P_S , the value $1/m$ represents a baseline failure probability: an informed adversary could simply guess the realized secret S uniformly at random from \mathcal{S} . To keep this failure probability below 1%, we set $|\mathcal{S}| = m = 128$ throughout this paper. We note that for a realistic adversary who does not know the specific subsets in \mathcal{S} , the complexity to reconstruct them from a high-entropy universe

U would be prohibitively high, rendering the failure probability to be $\ll 1/m$ in practice. While this potentially allows for a much smaller m , we adhere to the conservative choice of $m = 128$.

4.2.2 Mechanism Definition. At each time step t , the adversary observes the interaction transcript up to time t and submits a query input $q_t \in \mathcal{X}$ to the curator. We formally define the resulting mechanism $M_t : \mathcal{S} \rightarrow \mathbb{R}^d$ as $M_t(\cdot) = \hat{f}(q_t; \cdot)$, where $\hat{f}(x; D)$ denotes the prediction on $x \in \mathcal{X}$ made by a model trained on dataset $D \subseteq \mathcal{X} \times \mathcal{Y}$, which is a d -dimensional vector corresponding to the d classes.

Recall that the Gaussian noise in Theorem 2.5 and Definition 3.1 is calibrated to privatize deterministic functions M_t ; that is, the only source of randomness in the un-noised output $M_t(S)$ is the selection of the secret S itself. To achieve this, we explicitly derandomize the training and inference algorithms by fixing random seeds prior to execution. Note that these seeds can be made public without compromising the security game, as we consider a strong adversary knowing the learning and inference algorithms, whose uncertainty lies solely in the realization of the secret S .

We emphasize that aside from being deterministic, we impose no restrictions on the underlying training or inference algorithms. Our framework treats the training process as a general mechanism \hat{f} , which is agnostic to the choice of model architecture or optimization strategy. Any supervised learning algorithm can be employed to define \hat{f} ; crucially, this definition extends beyond simple model fitting. The function \hat{f} may encapsulate an entire learning pipeline, e.g., including hyperparameter tuning via cross-validation, architecture search, or automated model selection, provided these steps rely solely on the set S .

4.2.3 Computational Complexity. With P_S and M_t defined, Algorithm 1 is fully instantiated. As discussed in Section 3.2.2, a direct execution of the algorithm costs $O(mC + md^2)$ per query, where C is the cost of evaluating $M_t(S)$ for a single $S \in \mathcal{S}$. In our setting, $M_t(S) = \hat{f}(q_t; S)$ involves training a model on dataset S and then performing inference on q_t . Training m models for each query is computationally prohibitive for interactive systems.

However, we can significantly optimize this process by moving the training phase offline. Since the secret space $\mathcal{S} = \{S_1, \dots, S_m\}$ is fixed at initialization, we can train all m models $\{\hat{f}_1, \dots, \hat{f}_m\}$ in advance as a pre-processing step, where $\hat{f}_i : \mathcal{X} \rightarrow \mathbb{R}^d$ is the

model trained on S_i . During online interaction, evaluating the covariance matrix of M_t then reduces to running inference on the trained models, bringing the online per-query complexity down to $O(mC_{\text{infer}} + md^2)$, where C_{infer} is the cost of performing inference on a single model. We further note that the inference calls $\hat{f}_i(q_t)$ for $i = 1, \dots, m$ are embarrassingly parallelizable, which brings the effective per-query latency down to $O(C_{\text{infer}} + md^2)$ given sufficient computational resources. For comparison, under the non-private setting, inference costs $O(C_{\text{infer}})$, so our PAC-private mechanism incurs only an overhead of $O(md^2)$ per query in terms of latency, which is negligible compared to inference for modern ML models.

4.2.4 Output Stabilization. Typically, a learned classifier $\hat{f} : \mathcal{X} \rightarrow \mathbb{R}^d$ produces either *soft predictions* in the form of class probabilities (e.g., softmax scores) or *hard predictions* such as one-hot encoded labels. While softmax scores contain more information, their privatization would lead to significant utility loss due to instability. Recall that the noise level calibrated by Algorithm 1 is determined by the covariance matrix of the outputs $M_t(S)$ induced by a distribution P_t over the secret space \mathcal{S} , and the noise level is inversely proportional to the stability of the outputs. Continuous probability vectors often exhibit high variance across models trained on slightly different data, even when the predicted class is identical. This instability requires higher noise levels to meet the privacy budget. In contrast, discrete one-hot encodings are highly stable. For easy queries, the majority of models will predict the same class, resulting in identical outputs for most $S \in \mathcal{S}$. This minimizes variance across \mathcal{S} and requires significantly less noise to achieve the same privacy guarantee. Therefore, to maximize utility, we privatize the hard label predictions. After noise injection to the one-hot prediction to obtain response R_t , we take $\text{argmax}_i(R_t)$ as the final prediction. As we discuss in Section 5, this discrete structure also facilitates robust confidence filtering for downstream model distillation.

5 Model Distillation from Private Responses

While Algorithm 1 enables a large number of queries (cf. Table 1), the privacy budget is fundamentally finite and will be exhausted. Eventually, the accumulated leakage would exceed the pre-specified threshold and force the system to halt. To enable unlimited queries, we can distill a student model from the PAC-private responses. The quality of the resulting student model depends on the quality of the input queries and the label quality of the private responses; the latter depends on the intrinsic stability of the teacher model.

We can instantiate this given a large dataset $D_{\text{pub}} \subseteq \mathcal{X}$. This dataset does not need to be labeled, and may consist of public data or a pool of user queries collected while serving the private responses; the privatized labels on D_{pub} can be used to distill a student model. Since the curator does *not* use any additional information that the strong adversary does not know, the distilled student model inherits the rigorous PAC privacy via the post-processing inequality. Consequently, the student model (i.e., its weights) can be released for unlimited inference without incurring further privacy loss.

However, the injected noise introduces label errors that can degrade the utility of the student model. To mitigate this, we propose a confidence filtering step. Standard practice in model distillation filters samples based on the confidence scores returned by the

teacher model [23, 36, 49]. While our private responses lack interpretable confidence scores, we rely on the response structure that the underlying non-private prediction is a one-hot vector in \mathbb{R}^d and that the noise distribution (i.e., Σ) is known. This allows us to statistically test possible predictions against the observed noisy response. We note that this step is compatible with our threat model, as PAC privacy guarantees hold even when the adversary knows the privatized mechanism, which includes the noise distribution.

Given $x \in D_{\text{pub}}$, let $e_y = \hat{f}(x; S)$ be the non-private prediction, where $e_y \in \mathbb{R}^d$ is the y -th standard basis vector. Let $r = e_y + \mathcal{N}(0, \Sigma)$ be the observed private response and $\tilde{y} = \text{argmax}_i r_i$. To ensure label quality, we retain the sample (x, \tilde{y}) to train the student model only if the likelihood of \tilde{y} significantly exceeds that of *any other class* $j \neq \tilde{y}$. Formally, we use the following test to ensure that a mislabeled sample is retained with probability at most α .

PROPOSITION 5.1. *Given any significance level $\alpha \in (0, 1)$, we retain the sample (x, \tilde{y}) if and only if for all $j \neq \tilde{y}$:*

$$T_j(r) = \frac{(e_{\tilde{y}} - e_j)^\top \Sigma^{-1} (r - e_j)}{\sqrt{(e_{\tilde{y}} - e_j)^\top \Sigma^{-1} (e_{\tilde{y}} - e_j)}} \geq \Phi^{-1}(1 - \alpha),$$

where Φ^{-1} is the inverse CDF of the standard normal distribution. Then, the probability that (x, \tilde{y}) is retained while $\tilde{y} \neq y$ is at most α .

PROOF. $r \sim \mathcal{N}(e_y, \Sigma)$ with unknown e_y and known Σ . For any $j \neq \tilde{y}$, consider testing $H_0 : e_y = e_j$ vs $H_1 : e_y = e_{\tilde{y}}$. The test $T_j(r) \geq \Phi^{-1}(\alpha)$ has size α . Full proof is deferred to Appendix B.3. \square

Proposition 5.1 establishes a provable bound on the label noise: regardless of the ground-truth non-private prediction, the probability that our filtering mechanism falsely validates a private label altered by noise is at most α . This ensures that the student model is trained exclusively on high-confidence samples where the private response's signal is strong enough to statistically rule out all others.

6 Evaluation

6.1 Datasets and Models

We first give a brief overview of the datasets and models used throughout the experiments. We evaluate our framework on six standard classification benchmarks spanning tabular, computer vision, and natural language processing tasks.

- **Census Income** [2] is derived from the 1994 US Census. The task is to predict whether an individual's annual income exceeds \$50K from 15 categorical and continuous demographic attributes.
- **Bank Marketing** [28] contains marketing data of a Portuguese bank. The goal is to predict whether a client will subscribe to a term deposit based on 20 categorical and continuous features.
- **CIFAR-10** and **CIFAR-100** [21] are standard image benchmarks, consisting of $32 \times 32 \times 3$ images of 10 and 100 classes.
- **IMDb Reviews** [26] is a text dataset of highly polar movie reviews, and the task is to classify a review as positive or negative.
- **AG News** [53] is a text dataset comprising news articles from 4 categories: world, sports, business, and science/technology.

For the tabular datasets, we construct a random 80/20 train-test split. For the image and text datasets, we retain the original train-test splits from the sources. Key statistics of these datasets are summarized in Table 2. In our setup, the training split constitutes

Table 2: Summary of datasets used in our experiments, including modality, dataset sizes, and number of classes.

Dataset	Modality	Train	Test	Classes
Census Income [2]	Tabular	39,073	9769	2
Bank Marketing [28]	Tabular	32,950	8,238	2
CIFAR-10 [21]	Image	50,000	10,000	10
CIFAR-100 [21]	Image	50,000	10,000	100
IMDb Reviews [26]	Text	25,000	25,000	2
AG News [53]	Text	120,000	7,600	4

the universe U , and the secret training dataset S is sampled from this universe according to the prior distribution P_S . As described in Section 4.2.1, P_S is uniform over the $m = |\mathcal{S}| = 128$ subsets constructed such that $\forall u \in U, \Pr(u \in S) = 1/2$. In expectation, each set in \mathcal{S} contains half the data of the universe U .

Since our privacy framework is model-agnostic, we can employ any ML pipeline to train the model on the secret dataset S as an instantiation of $\hat{f}(\cdot; S)$, as discussed in Section 4.2.2. For tabular datasets, we utilize XGBoost [5]. To optimize performance, we perform a hyperparameter sweep and choose the best combination via cross-validation on S . For image classification, we use the Wide-ResNet-28-10 architecture [51], a standard choice in recent DP literature [8, 39]. This model has 36.5 million parameters and is designed for CIFAR-style $32 \times 32 \times 3$ images. We train the model using standard data pre-processing and hyperparameters. Additionally, as S is a subsampled subset of U with expectedly half the size, we apply CutMix [50] and MixUp [52] for augmentation. For text classification, we train a BERT-Small model [11, 41] from scratch, which is a compact variant of BERT with 28.8 million parameters. We reserve 10% of S as a validation set for early stopping. Our code is available at https://github.com/zhxchd/pac_private_responses, and implementation details are provided in Appendix C.

6.2 PAC-Private Responses

To evaluate the privacy and utility of our proposed framework, we experiment with the private response mechanism described in Section 4 on each of the six datasets. As a one-time pre-processing step, we sample $m = 128$ subsets to fix the prior P_S and train a model on each subset. We then run 1,000 independent trials. In each trial, we submit a random permutation of test examples to query our private response mechanism and report the average accuracy.

We test our mechanism under a wide range of per-step MI budgets b , ranging from 2^{-4} down to 2^{-32} . In this interactive setting, we deliberately do not fix a total MI budget B to be allocated over all test examples, because doing so would implicitly tie the overall privacy guarantee to the size of the test data. Instead, our goal is to support a large number of queries, potentially far exceeding the size of the test dataset, and the overall privacy guarantee depends on the total number of queries T . Therefore, we treat b as the primary security parameter: the cumulative privacy guarantee follows as a function of b and the total number of queries T . A data curator can consult Table 1 to select an appropriate value of b based on their expected query volume and desired privacy target. For example, to

bound MIA success by 51.08% after one million queries, one can set $b = 2^{-32}$. In Section 6.3, we further report the empirical MIA success rates. Additionally, we include two non-private baselines. First, we run our private response mechanism with b set to infinity. In this case, the predictions are still made by the model trained on the secret dataset S sampled from P_S , but no noise is added. Finally, we also report the non-private baseline for a model directly trained on the full universe U . The results are presented in Table 3.

Privacy-Utility Trade-off. Utility loss in our frameworks originates from two sources: subsampling and noise injection. That is, to enable PAC privatization, our mechanism trains the underlying model on a secret dataset S subsampled from U . This results in a *subsampling* error, captured by the performance gap between the non-private and $b = \infty$ baselines in Table 3. For all datasets, this gap is minimal (< 2%), with the only exception of CIFAR-100, where the small number of samples (i.e., merely 500) per class makes the effects of subsampling more significant. Second, noise injection further degrades the utility as the budget b tightens.

We observe a surprising phenomenon: rather than collapsing to triviality, the utility converges even as b tightens to extremely small values. As shown in Table 3, accuracy remains nearly constant as b decreases from 2^{-16} to 2^{-32} , and our mechanism maintains strong utility even at $b = 2^{-32}$ for all datasets. This resilience is a direct consequence of the instance-dependent nature of PAC privacy. When the responses are stable — that is, when most of the underlying models trained on different $S \in \mathcal{S}$ agree on the prediction for a given input — the mutual information is inherently low. Consequently, the mechanism can satisfy extremely strict per-step privacy bounds with minimal noise, preserving strong utility even when b is vanishingly small. Notably, this is only true when responses are in the form of one-hot vectors. Confidence scores themselves are often much less stable, as discussed in Appendix D.1.

An effective local proxy for such stability is the subsampling error. Small subsampling error implies generalizability — that is, the subsampled dataset is representative of the population, and the model trained on a subsampled dataset generalizes well beyond its training data. This further suggests that models trained on *different* subsets are also likely to converge to similar decision boundaries, thereby exhibiting high stability and requiring less noise to hide the secret set. This correlation is evident in our results. For the two tabular datasets, where the tasks are simpler and data is abundant, the subsampling gap is negligible (< 0.3%). Consequently, the predictions are highly stable across the m models, and we observe almost no utility drop at $b = 2^{-32}$ as compared to the non-private baseline. In contrast, CIFAR-100 exhibits a larger subsampling penalty from 84.02% to 77.79%. This indicates larger variance and thus, noise for privatization, leading to a more significant utility drop at $b = 2^{-32}$ (down to 56.15%). Nevertheless, this performance remains competitive compared to standard DP baselines. Crucially, this suggests that a model that generalizes well and exhibits low variance will naturally incur a lower utility cost under PAC privacy, alluding to “win-win” scenarios between robust learning and privacy.

Comparisons to DP. We note that applying DP directly to the prediction outputs is generally infeasible in our setup. That is, without strong assumptions on the learner’s stability which cannot be established for our complex, non-convex models, excessive noise

Table 3: Average test accuracy (%) of PAC-private responses under various per-step mutual information budgets $2^{-32} \leq b \leq 2^{-4}$ across datasets. See Table 1 on the provable upper bounds on MIA success for each b after varying numbers of responses. For all datasets, even when the per-step MI budget b is as tight as 2^{-32} , the private responses maintain strong utility.

Modality	Dataset	Non-Private	$b = \infty$	$b = 2^{-4}$	$b = 2^{-8}$	$b = 2^{-12}$	$b = 2^{-16}$	$b = 2^{-20}$	$b = 2^{-24}$	$b = 2^{-28}$	$b = 2^{-32}$
Tabular	Census Income	87.39	87.17	87.15	86.68	85.92	85.86	85.84	85.84	85.84	85.84
	Bank Marketing	91.98	91.69	91.67	91.02	90.36	90.28	90.28	90.27	90.27	90.29
Image	CIFAR-10	97.37	95.80	95.71	93.52	88.35	87.90	87.81	87.80	87.80	87.79
	CIFAR-100	84.02	77.79	77.69	75.56	58.38	56.34	56.17	56.13	56.10	56.11
Text	IMDb Reviews	87.10	85.13	85.13	84.46	74.26	69.32	69.16	69.09	69.10	69.10
	AG News	91.61	90.44	90.35	87.95	80.18	79.42	79.31	79.27	79.25	79.25

based on worst-case sensitivity is necessary [14]. On the other hand, practical protocols like PATE [30, 32] are designed for semi-supervised learning rather than functioning as a continuous prediction service (see Section 7 for details). Therefore, standard practice for differentially-private ML usually involves privatizing model weights via algorithms like DP-SGD [1, 37], which often incurs substantial utility loss in practice. The state-of-the-art result for private image classification [39] achieves an accuracy of 72.32% on CIFAR-10 at $\epsilon = 1$ and 43.33% on CIFAR-100 at $\epsilon = 3$. In contrast, our response-based mechanism achieves significantly higher utility even under stricter privacy accounting. At a per-query budget of $b = 2^{-32}$, our method supports approximately 477 million queries before the accumulated leakage reaches an equivalent of $\epsilon = 1$, and over 2 billion queries for $\epsilon = 3$, while maintaining higher accuracies of 87.76% for CIFAR-10 and 56.15% for CIFAR-100, respectively.

The reason that our method enjoys a more desirable privacy-utility trade-off is two-fold. First, we operate under a relaxed threat model: we privatize *responses* behind an API rather than publishing the *weights* of the model trained on the realized secret set S . More importantly, PAC privacy is *instance-dependent*. Unlike DP, which must calibrate noise to the worst-case input-independent sensitivity, PAC privacy exploits the stability of the underlying task, adding negligible noise when the response is stable across possible training datasets. While our approach does not replace DP-SGD for use cases requiring model releases, it offers a more favorable privacy-utility trade-off for ML inference services where the threat model aligns with ours. We further highlight the benefit of input-dependence in Section 6.4, by comparing our distilled models against DP-SGD fine-tuning baselines, where both models are publishable.

6.3 Defense Against MIA

To empirically evaluate the privacy of our algorithms, we must execute membership inference attacks under our threat model. Standard MIA literature typically assumes an adversary with limited knowledge. As a result, they often rely on heuristic attacks, such as training shadow models to *estimate* the behavior of the target model and setting threshold-based criteria for membership [4, 35]. However, under our threat model, where the strong adversary possesses full knowledge of the distribution P_S of the secret and functions M_t , heuristic approximation is not necessary. The adversary can derive the optimal strategy to maximize their success rate for a given transcript. We formally characterize this optimal attack below.

PROPOSITION 6.1 (OPTIMAL MIA DECISION RULE). *Let random variable \mathcal{T}_T be the transcript of interactions up to time T . For a target individual $u^* \in U$, the decision rule $A : \text{supp}(\mathcal{T}_T) \rightarrow \{0, 1\}$ that maximizes the adversary’s membership inference accuracy is:*

$$A^*(\tau_T) = \begin{cases} 1 & \text{if } \sum_{S \in \mathcal{S}} \mathbb{1}\{u^* \in S\} \cdot P(S \mid \mathcal{T}_T = \tau_T) > 0.5 \\ 0 & \text{otherwise} \end{cases}. \quad (5)$$

PROOF. This follows from the derivation of a Bayes optimal statistical procedure. Full proof is deferred to Appendix B.4. \square

Remark 6.2. Proposition 6.1 defines the optimal *inference* strategy after observing $\mathcal{T}_T = \tau_T$. It does not, however, describe the optimal strategy for *choosing* the queries q_t . While the adversary can adaptively select q_t to maximize the expected information gain, solving for the optimal query sequence is computationally intractable.

In our experiments, the adversary seeks to simultaneously infer the membership of all examples in the universe U , i.e., to decide whether $u \in U$ belongs to the realized secret set S used for responses. Following standard MIA protocols [4, 35], the adversary queries the mechanism using the exact examples from U whose membership they wish to discover. Crucially, because the adversary has full system knowledge and $m = |\mathcal{S}|$ is tractable, they can evaluate Eq. (5) exactly. This step mirrors the belief state update performed by the curator in Algorithm 1. We execute 1,000 independent trials. In each trial, we submit a sequence of up to one million queries, randomly sampled from U without replacement. At various time steps T , we run the optimal decision rule Eq. (5) to infer the membership of all examples in U and report the average accuracy.

MIA results on CIFAR-10 are summarized in Table 4. Under $2^{-24} \leq b \leq 2^{-12}$, we observe a clear improvement in the empirical MIA accuracy with more queries. When the per-step MI budget is vanishingly small, i.e., $b = 2^{-28}$ or 2^{-32} , the adversary struggles to achieve non-trivial membership inference even after one million queries. Notably, across all settings, the empirical MIA accuracy is *strictly bounded* by the theoretical guarantees derived by PAC privacy, often with a significant gap. For instance, at $b = 2^{-12}$, any query volume above 10,000 results in a vacuous theoretical guarantee of 100%, yet the adversary only achieves perfect membership inference after 600,000 queries. This parallels findings in DP, where larger privacy budgets (i.e., ϵ) provide loose MIA upper bounds, while often effectively defending against empirical attacks [19, 25].

Table 4: Upper bounds of MIA success and the average MIA accuracy of Proposition 6.1 after T PAC-private responses on CIFAR-10 at different levels of per-step MI budget b . Empirical MIA accuracy is strictly bounded by the theoretical guarantee.

Number of Responses T	100,000	200,000	300,000	400,000	500,000	600,000	700,000	800,000	900,000	1,000,000
$b = 2^{-12}$	MIA Bound (%)	100.00	100.00	100.00	100.00	100.00	100.00	100.00	100.00	100.00
	MIA Acc (%)	74.17	90.00	97.14	99.55	99.95	100.00	100.00	100.00	100.00
$b = 2^{-16}$	MIA Bound (%)	100.00	100.00	100.00	100.00	100.00	100.00	100.00	100.00	100.00
	MIA Acc (%)	53.02	54.34	55.68	57.18	58.23	59.74	61.31	62.44	64.18
$b = 2^{-20}$	MIA Bound (%)	71.48	79.85	85.89	90.60	94.38	97.39	99.61	100.00	100.00
	MIA Acc (%)	50.75	50.99	51.19	51.47	51.76	52.00	52.13	52.28	52.39
$b = 2^{-24}$	MIA Bound (%)	55.45	57.71	59.43	60.87	62.15	63.29	64.34	65.32	66.23
	MIA Acc (%)	50.09	50.17	50.35	50.25	50.24	50.36	50.40	50.41	50.47
$b = 2^{-28}$	MIA Bound (%)	51.36	51.93	52.36	52.73	53.05	53.34	53.61	53.86	54.09
	MIA Acc (%)	49.96	50.03	50.07	50.08	50.01	49.96	49.99	50.02	50.01
$b = 2^{-32}$	MIA Bound (%)	50.34	50.48	50.59	50.68	50.76	50.84	50.90	50.97	51.02
	MIA Acc (%)	50.05	50.00	49.88	49.85	49.86	49.88	49.90	49.94	49.90

Table 5: Average CIFAR-10 test accuracy of a model distilled from T private responses to CINIC-ImageNet examples. Trained on 210,000 responses, the distilled model achieves 91.86% accuracy, while provably bounding the MIA success to 50.49%, the same as $(0.0198, 10^{-5})$ -DP. For context, the SoTA result of DP-SGD fine-tuning on CIFAR-10 achieves 94.7% accuracy at $\epsilon = 1$ [8].

Number of Responses (T)	5,000	10,000	20,000	40,000	80,000	160,000	210,000
Total MI Budget (B_T)	1.16×10^{-6}	2.33×10^{-6}	4.66×10^{-6}	9.31×10^{-6}	1.86×10^{-5}	3.73×10^{-5}	4.89×10^{-5}
MIA Success Rate Bound (%)	50.08	50.11	50.15	50.22	50.31	50.43	50.49
DP ϵ w/ Matching Guarantee ($\delta = 10^{-5}$)	0.0030	0.0043	0.0061	0.0086	0.0122	0.0172	0.0198
Avg. Number of Confident Responses	1,989	3,976	7,951	15,983	32,070	64,136	84,295
Avg. Distilled Model Test Accuracy (%)	64.01	69.79	81.34	84.94	87.74	91.19	91.86

This disparity between the theoretical guarantee and the empirical accuracy of MIA can be attributed to the adversary’s suboptimal querying strategy. As noted in Remark 6.2, while Proposition 6.1 derives the *optimal inference rule* after observing the transcript, it does not characterize the *optimal querying strategy* to select each q_t . While querying examples from U is a standard practice in MIA literature, an adversary could use more complex strategies. For instance, recent work [33, 42] suggests that adversarially generated examples can efficiently extract membership information. While our empirical attack employs a more straightforward querying strategy, we note that our theoretical guarantee provides provable privacy bounds under *any possible querying strategy*.

6.4 Private Model Distillation

To evaluate the distillation protocol described in Section 5, we simulate a scenario where the curator uses the private response mechanism to label a large auxiliary dataset. As a proof of concept, we use the ImageNet partition of the CINIC-10 dataset [7] as our auxiliary dataset; while it shares the same 10 classes as CIFAR-10, it represents a distinct distribution. This mimics realistic deployment settings where the distillation data may be collected from user queries, or curated from public sources. We restrict this experiment

to CIFAR-10; to the best of our knowledge, there are no similar auxiliary datasets for the other datasets. We use all 210,000 examples in the CINIC-ImageNet dataset to query the private response mechanism trained on CIFAR-10, under a strict per-step budget of $b = 2^{-32}$. To ensure the quality of the distillation data, we apply confidence filtering (cf. Proposition 5.1) with a significance level $\alpha = 0.01$. The accepted samples, with their privacy-preserving labels, are then used to train a Wide-ResNet-28-10 model from scratch. We run this distillation process 5 times and report the average results.

The private responses trained on CIFAR-10 achieve an accuracy of 58.66% on the ImageNet examples, as a result of distribution shift. However, our confidence filtering proves highly effective in practice: it retains $\approx 40\%$ of the privately labeled auxiliary examples, and the accuracy on this subset rises dramatically to over 95%. This confirms that the hypothesis test successfully isolates high-quality, in-distribution examples from the noisy, out-of-distribution data.

The accuracy of the distilled student model on CIFAR-10 test examples is summarized in Table 5. First, we notice that the distillation utility is strong even with limited auxiliary data. With only 5,000 queries, the student trained on merely 1,989 confident examples already achieves 64.01% accuracy. Using all 210,000 queries, the distilled model achieves 91.86% accuracy. Notably, this outperforms the private teacher itself with 87.79% accuracy, as the student effectively learns from the diverse features in the ImageNet examples with

high-quality private labels. This highlights that proper distillation can unlock utility beyond the private responses’ baseline.

From a privacy perspective, releasing this student model exposes only the information leaked through the 210,000 private responses about membership of the CIFAR-10 examples. The accumulated MI bound corresponds to an upper bound of 50.49% on MIA success, which offers a privacy guarantee comparable to $\epsilon \approx 0.02$ under DP. We compare this to the standard setting of differentially private fine-tuning, which similarly assumes public access to additional data and protects only the fine-tuning dataset. The state-of-the-art result under this setting achieves 94.7% accuracy on CIFAR-10 at $\epsilon = 1$ [8] when fine-tuning a Wide-ResNet-28-10 model pre-trained on ImageNet [10]. Our method achieves slightly worse utility (91.86%) while offering a privacy guarantee that is orders of magnitude tighter. Further, our distillation protocol does not require the public dataset to be labeled, which is particularly favorable in scenarios where large-scale, unlabeled public data is available.

7 Related work

Differential Privacy. Conventionally, privacy-preserving ML focuses on releasing differentially private model weights, most commonly via DP-SGD, which clips per-sample gradients to bound sensitivity and injects noise during optimization [1, 37]. However, this approach often incurs substantial utility loss, particularly on larger models. A recent survey [9] emphasizes that DP in deep learning is fundamentally challenged by the high-dimensionality of the model. As a result, competitive utility under DP is often achieved either with relaxed privacy budgets, or relying on public data. This is evident in private image classification. Tramèr and Boneh [40] show that lower dimensional classifiers on fixed features often outperform end-to-end DP training. De et al. [8] demonstrate that scaling and careful tuning improve DP-SGD performance, yet strong utility at tight budgets ($\epsilon \approx 1$) is achieved primarily via fine-tuning pretrained models. More recently, Tang et al. [39] push the training-from-scratch utility of DP-SGD by learning priors generated from random processes. This achieves the SoTA accuracy of 72.32% on CIFAR-10 at $\epsilon = 1$ and 43.33% on CIFAR-100 at $\epsilon = 3$, still far from non-private baselines. Finally, a recent benchmark [27] explicitly separates settings with and without public data and highlights that large public pretraining is crucial for competitive utility.

To bypass this curse of dimensionality, a parallel line of work explores *private prediction*, where DP is enforced on the sequence of outputs rather than the model itself. Dwork and Feldman [14] establish the theoretical foundation for this setting and formalize the link between algorithmic stability and privacy. However, this framework relies on strong assumptions regarding the learner’s stability to bound sensitivity, typically only provable for simple or convex learners. Without such assumption, private prediction must rely on pessimistic sensitivity bounds (e.g., the diameter of the output space), resulting in excessive noise. In parallel, PATE [30, 32] proposes a practical approach to private prediction via architectural design. By training k teacher models on disjoint data partitions, PATE bounds sensitivity by ensuring each data point only affects a single teacher’s vote. Predictions agreed upon by the teacher models are used to train a student that inherits the DP guarantee. However, PATE has important limitations as a general-purpose

private response mechanism. First, its privacy guarantees typically require data-dependent accounting, with per-query privacy loss determined by teacher vote margins, making the total number of answerable queries hard to bound a priori. Moreover, disjoint partitioning introduces a scaling dilemma: increasing k to reduce per-query privacy cost simultaneously reduces the data available to each teacher, weakening consensus and degrading utility. Fundamentally, PATE does not calibrate noise to the inherent *instance-dependent stability* of the teacher models, but instead enforces a sensitivity bound strictly through the architectural construction of k disjoint partitions. As a result, PATE is most effective as a semi-supervised private learning algorithm, rather than as a standalone private prediction mechanism to answer a large number of queries.

PAC Privacy. While DP has been the de facto standard for provable privacy protection, various relaxations have been explored to achieve meaningful privacy-utility trade-offs. We consider PAC privacy [44, 45] as a compelling addition to this area. While DP provides strong, input-independent guarantees corresponding to *individual privacy*, PAC privacy provides *instance-based* guarantees. Specifically, the secret protected in PAC privacy is the specific realization sampled from a known data distribution, typically instantiated through a subsampling-based approach.

Xiao and Devadas [44] first established the theoretical foundations of this framework, demonstrating that PAC privacy allows for the privatization of arbitrary black-box functions via simulations. Subsequent works apply PAC privacy for learnable encryption [46] and classical machine learning algorithms such as k-means, SVM, and decision trees [38]. The latter work explicitly links utility under PAC privacy to algorithmic stability. However, these applications operate under a single release. Composition under PAC privacy is first explored by Xiao and Devadas [44], who provided a simple linear composition theorem under the *non-adaptive* setting. More recently, Xiao [43] attempts to extend these results to the adaptive and adversarial setting. However, this extension effectively enforces a DP-like input-independent bound to handle adaptivity, negating the core benefits of PAC privacy. Our work addresses this by providing tight instance-based composition under the adversarial setting.

8 Conclusion

This work presented a novel framework to release PAC-private responses under adaptive and adversarial queries. We derived a novel adversarial composition theorem for PAC privacy that achieves tight privacy accounting via *adaptive noise calibration* to adjust to the adversary’s shifting beliefs. Instantiated for ML predictions, our method exploits the inherent stability of model responses and maintains high utility under tight privacy budgets.

Potential future directions include theoretical extensions of our composition theory, such as privacy accounting under f -divergence and efficient estimation for intractable secret spaces. Another promising avenue is applying response privacy to LLM inference [16, 18]. Finally, Algorithm 1 is a general-purpose tool applicable to any iterative algorithms with sequential, adaptive releases, such as SGD.

References

- [1] Martín Abadi, Andy Chu, Ian J. Goodfellow, H. Brendan McMahan, Ilya Mironov, Kunal Talwar, and Li Zhang. 2016. Deep Learning with Differential Privacy. In

Proceedings of the 2016 ACM SIGSAC Conference on Computer and Communications Security. 308–318.

[2] Barry Becker and Ronny Kohavi. 1996. Adult. UCI Machine Learning Repository. DOI: <https://doi.org/10.24432/C5XW20>.

[3] Leo Breiman. 2001. Statistical modeling: The two cultures (with comments and a rejoinder by the author). *Statist. Sci.* 16, 3 (2001), 199–231.

[4] Nicholas Carlini, Steve Chien, Milad Nasr, Shuang Song, Andreas Terzis, and Florian Tramèr. 2022. Membership Inference Attacks From First Principles. In *43rd IEEE Symposium on Security and Privacy*. 1897–1914.

[5] Tianqi Chen and Carlos Guestrin. 2016. XGBoost: A Scalable Tree Boosting System. In *Proceedings of the 22nd ACM SIGKDD International Conference on Knowledge Discovery and Data Mining*. 785–794.

[6] Alexander D’Amour, Katherine A. Heller, Dan Moldovan, Ben Adlam, Babak Alipanahi, Alex Beutel, Christina Chen, Jonathan Deaton, Jacob Eisenstein, Matthew D. Hoffman, Farhad Hormozdiari, Neil Houlsby, Shaobo Hou, Ghassen Jerfel, Alan Karthikresalingam, Mario Lucic, Yi-An Ma, Cory Y. McLean, Diana Minciuc, Akinori Mitani, Andrea Montanari, Zachary Nado, Vivek Natarajan, Christopher Nielson, Thomas F. Osborne, Rajiv Raman, Kim Ramasamy, Rory Sayres, Jessica Schrouff, Martin Seneviratne, Shannon Sequeira, Harini Suresh, Victor Veitch, Max Vladymyrov, Xuezhi Wang, Kelli Webster, Steve Yadlowsky, Taedong Yun, Xiaohui Zhai, and D. Sculley. 2022. Underspecification Presents Challenges for Credibility in Modern Machine Learning. *J. Mach. Learn. Res.* 23 (2022), 226:1–226:61.

[7] Luke N. Darlow, Elliot J. Crowley, Antreas Antoniou, and Amos J. Storkey. 2018. CINIC-10 is not ImageNet or CIFAR-10. arXiv:1810.03505

[8] Soham De, Leonard Berrada, Jamie Hayes, Samuel L. Smith, and Borja Balle. 2022. Unlocking High-Accuracy Differentially Private Image Classification through Scale. arXiv:2204.13650

[9] Lea Demelius, Roman Kern, and Andreas Trügler. 2025. Recent Advances of Differential Privacy in Centralized Deep Learning: A Systematic Survey. *ACM Comput. Surv.* 57, 6 (2025), 158:1–158:28.

[10] Jia Deng, Wei Dong, Richard Socher, Li-Jia Li, Kai Li, and Li Fei-Fei. 2009. ImageNet: A large-scale hierarchical image database. In *2009 IEEE Computer Society Conference on Computer Vision and Pattern Recognition*. 248–255.

[11] Jacob Devlin, Ming-Wei Chang, Kenton Lee, and Kristina Toutanova. 2019. BERT: Pre-training of Deep Bidirectional Transformers for Language Understanding. In *Proceedings of the 2019 Conference of the North American Chapter of the Association for Computational Linguistics: Human Language Technologies*. 4171–4186.

[12] John C. Duchi, Michael I. Jordan, and Martin J. Wainwright. 2013. Local Privacy and Statistical Minimax Rates. In *54th Annual IEEE Symposium on Foundations of Computer Science*. 429–438.

[13] Cynthia Dwork. 2006. Differential Privacy. In *33rd International Colloquium on Automata, Languages and Programming*, Vol. 4052. 1–12.

[14] Cynthia Dwork and Vitaly Feldman. 2018. Privacy-preserving Prediction. In *Conference On Learning Theory (Proceedings of Machine Learning Research)*, Vol. 75. 1693–1702.

[15] Cynthia Dwork and Aaron Roth. 2014. The Algorithmic Foundations of Differential Privacy. *Found. Trends Theor. Comput. Sci.* 9, 3–4 (2014), 211–407.

[16] James Flemings, Meisam Razaviyayn, and Murali Annavaram. 2024. Differentially Private Next-Token Prediction of Large Language Models. In *Proceedings of the 2024 Conference of the North American Chapter of the Association for Computational Linguistics: Human Language Technologies (Volume 1: Long Papers)*. 4390–4404.

[17] Wensheng Gan, Shicheng Wan, and Philip S. Yu. 2023. Model-as-a-Service (MaaS): A Survey. In *IEEE International Conference on Big Data*. 4636–4645.

[18] Antonio Ginart, Laurens van der Maaten, James Zou, and Chuan Guo. 2022. Submix: Practical Private Prediction for Large-Scale Language Models. arXiv:2201.00971

[19] Bargav Jayaraman and David Evans. 2019. Evaluating Differentially Private Machine Learning in Practice. In *28th USENIX Security Symposium*. 1895–1912.

[20] Bo Jiang, Wanrong Zhang, Donghang Lu, Jian Du, Sagar Sharma, and Qiang Yan. 2025. Meeting Utility Constraints in Differential Privacy: A Privacy-Boosting Approach. In *IEEE Symposium on Security and Privacy*. 3931–3949.

[21] Alex Krizhevsky. 2009. *Learning Multiple Layers of Features from Tiny Images*. Technical Report. University of Toronto. <https://www.cs.toronto.edu/~kriz/learning-features-2009-TR.pdf>

[22] Alex Krizhevsky, Ilya Sutskever, and Geoffrey E. Hinton. 2012. ImageNet Classification with Deep Convolutional Neural Networks. In *Advances in Neural Information Processing Systems 25: 26th Annual Conference on Neural Information Processing Systems 2012*. 1106–1114.

[23] Dong-Hyun Lee. 2013. Pseudo-label: The simple and efficient semi-supervised learning method for deep neural networks. In *ICML 2013 Workshop: Challenges in Representation Learning*.

[24] Ilya Loshchilov and Frank Hutter. 2019. Decoupled Weight Decay Regularization. In *7th International Conference on Learning Representations*.

[25] Andrew Lowy, Zhuohang Li, Jing Liu, Toshiaki Koike-Akino, Kieran Parsons, and Ye Wang. 2024. Why Does Differential Privacy with Large Epsilon Defend Against Practical Membership Inference Attacks? arXiv:2402.09540

[26] Andrew L. Maas, Raymond E. Daly, Peter T. Pham, Dan Huang, Andrew Y. Ng, and Christopher Potts. 2011. Learning Word Vectors for Sentiment Analysis. In *The 49th Annual Meeting of the Association for Computational Linguistics: Human Language Technologies*. 142–150.

[27] Sabrina Mokhtari, Sara Kodeiri, Shubhankar Mohapatra, Tramèr, and Gautam Kamath. 2025. Rethinking Benchmarks for Differentially Private Image Classification. *IEEE Data Eng. Bull.* 4 (2025), 137–156.

[28] S. Moro, P. Rita, and P. Cortez. 2014. Bank Marketing. UCI Machine Learning Repository. DOI: <https://doi.org/10.24432/C5K306>.

[29] OECD. 2024. AI, data governance and privacy: Synergies and areas of international co-operation. *OECD Artificial Intelligence Papers* 20 (2024).

[30] Nicolas Papernot, Martin Abadi, Úlfar Erlingsson, Ian J. Goodfellow, and Kunal Talwar. 2017. Semi-supervised Knowledge Transfer for Deep Learning from Private Training Data. In *5th International Conference on Learning Representations*.

[31] Nicolas Papernot, Patrick D. McDaniel, Arunesh Sinha, and Michael P. Wellman. 2018. SoK: Security and Privacy in Machine Learning. In *2018 IEEE European Symposium on Security and Privacy*. 399–414.

[32] Nicolas Papernot, Shuang Song, Ilya Mironov, Ananth Raghunathan, Kunal Talwar, and Úlfar Erlingsson. 2018. Scalable Private Learning with PATE. In *6th International Conference on Learning Representations*.

[33] Yuefeng Peng, Jaechul Roh, Subhransu Maji, and Amir Houmansadr. 2024. OSLO: One-Shot Label-Only Membership Inference Attacks. In *Advances in Neural Information Processing Systems* 38.

[34] Reza Shokri and Vitaly Shmatikov. 2015. Privacy-Preserving Deep Learning. In *Proceedings of the 22nd ACM SIGSAC Conference on Computer and Communications Security*. 1310–1321.

[35] Reza Shokri, Marco Stronati, Congzheng Song, and Vitaly Shmatikov. 2017. Membership Inference Attacks Against Machine Learning Models. In *2017 IEEE Symposium on Security and Privacy*. 3–18.

[36] Kihyuk Sohn, David Berthelot, Nicholas Carlini, Zizhao Zhang, Han Zhang, Colin Raffel, Ekin Dogus Cubuk, Alexey Kurakin, and Chun-Liang Li. 2020. FixMatch: Simplifying Semi-Supervised Learning with Consistency and Confidence. In *Advances in Neural Information Processing Systems 33: Annual Conference on Neural Information Processing Systems 2020*.

[37] Shuang Song, Kamalika Chaudhuri, and Anand D. Sarwate. 2013. Stochastic gradient descent with differentially private updates. In *IEEE Global Conference on Signal and Information Processing*. 245–248.

[38] Mayuri Sridhar, Hanshen Xiao, and Srinivas Devadas. 2025. PAC-Private Algorithms. In *IEEE Symposium on Security and Privacy*. 3839–3857.

[39] Xinyu Tang, Ashwinee Panda, Vikash Sehwag, and Prateek Mittal. 2025. Differentially Private Image Classification by Learning Priors from Random Processes. *J. Priv. Confidentiality* 15, 1 (2025).

[40] Florian Tramèr and Dan Boneh. 2021. Differentially Private Learning Needs Better Features (or Much More Data). In *9th International Conference on Learning Representations*.

[41] Iulia Turc, Ming-Wei Chang, Kenton Lee, and Kristina Toutanova. 2019. Well-Read Students Learn Better: On the Importance of Pre-training Compact Models. arXiv:1908.08962

[42] Yutong Wu, Han Qiu, Shangwei Guo, Jiwei Li, and Tianwei Zhang. 2024. You Only Query Once: An Efficient Label-Only Membership Inference Attack. In *The Twelfth International Conference on Learning Representations*.

[43] Hanshen Xiao. 2024. *Automated and Provable Privatization for Black-Box Processing*. Ph. D. Dissertation. Massachusetts Institute of Technology.

[44] Hanshen Xiao and Srinivas Devadas. 2023. PAC Privacy: Automatic Privacy Measurement and Control of Data Processing. In *Advances in Cryptology – CRYPTO 2023*, Vol. 14082. 611–644.

[45] Hanshen Xiao and Srinivas Devadas. 2025. PAC Privacy and Black-Box Privatization. *IEEE Secur. Priv.* 23, 4 (2025), 92–97.

[46] Hanshen Xiao, G. Edward Suh, and Srinivas Devadas. 2024. Formal Privacy Proof of Data Encoding: The Possibility and Impossibility of Learnable Encryption. In *Proceedings of the 2024 on ACM SIGSAC Conference on Computer and Communications Security*. 1834–1848.

[47] Hanshen Xiao, Jun Wan, Elaine Shi, and Srinivas Devadas. 2025. One-Sided Bounded Noise: Theory, Optimization Algorithms and Applications. In *Proceedings of the 2025 ACM SIGSAC Conference on Computer and Communications Security*. 4214–4228.

[48] Xiaokui Xiao and Yufei Tao. 2008. Output perturbation with query relaxation. *Proc. VLDB Endow.* 1, 1 (2008), 857–869.

[49] Qizhe Xie, Minh-Thang Luong, Eduard H. Hovy, and Quoc V. Le. 2020. Self-Training With Noisy Student Improves ImageNet Classification. In *2020 IEEE/CVF Conference on Computer Vision and Pattern Recognition*. 10684–10695.

[50] Sangdoo Yun, Dongyoon Han, Sanghyuk Chun, Seong Joon Oh, Youngjoon Yoo, and Junsuk Choe. 2019. CutMix: Regularization Strategy to Train Strong Classifiers With Localizable Features. In *2019 IEEE/CVF International Conference on Computer Vision*. 6022–6031.

[51] Sergey Zagoruyko and Nikos Komodakis. 2016. Wide Residual Networks. In *Proceedings of the British Machine Vision Conference 2016*.

[52] Hongyi Zhang, Moustapha Cissé, Yann N. Dauphin, and David Lopez-Paz. 2018. mixup: Beyond Empirical Risk Minimization. In *6th International Conference on Learning Representations*.

[53] Xiang Zhang, Junbo Jake Zhao, and Yann LeCun. 2015. Character-level Convolutional Networks for Text Classification. In *Advances in Neural Information Processing Systems 28*. 649–657.

A Analysis of Static Adversarial Composition

We hereby provide a more detailed analysis of the static adversarial composition [43] briefly discussed in Section 3.2. We first state the formal composition theorem for this algorithm.

THEOREM A.1 ([43]). *Consider the same setting described in Section 3.1. If at each step $t = 1, 2, \dots, T$, the noise covariance matrix Σ_t is calibrated w.r.t. P_S and M_t to enforce the following bounds:*

$$\sup_Q I_{S \sim Q}(S; M_t(S) + \mathcal{N}(0, \Sigma_t)) \leq b'_t, \quad (6)$$

$$I_{S \sim P_S}(S; M_t(S) + \mathcal{N}(0, \Sigma_t)) \leq b_t, \quad (7)$$

Then, the overall mutual information leakage after T steps is bounded as follows:

$$I(S; R_1, \dots, R_T) \leq B_T, \quad (8)$$

where $B_1 = b_1$ and for $t \geq 2$,

$$B_t = B_{t-1} + \min\{b'_t \sqrt{2B_{t-1}} + b_t, b'_t\}.$$

PROOF. Please refer to Theorem 4.2 and Appendix A.8 of [43]. \square

We note that the first constraint Eq. (6) is an input-independent worst-case guarantee that is similar to the *sensitivity* for local differential privacy [12], while the second constraint Eq. (7) is the standard mutual information bound we enforce with regard to the specific choice of P_S and M_t .

Assuming a uniform budget allocation $b_t = b$ and $b'_t = b'$ for all t , the recurrence relation of the cumulative MI bound is

$$B_t = B_{t-1} + \min\{b', b + b' \sqrt{2B_{t-1}}\},$$

where $B_1 = b_1$. We consider two scenarios for the choice of b' relative to b .

First, if b' is set such that $b' \approx b$, then $B_T = b'T$ scales linearly in T . However, enforcing such a small b' requires the noise Σ_t to be calibrated to the worst-case capacity of the channel (i.e., Eq. (6)), rendering the instance-specific bound (i.e., Eq. (7)) redundant. This ignores the stability of M_t under P_S and results in a significantly higher noise level, effectively reverting to a DP-style guarantee based on *sensitivity* rather than *average-case stability*. This negates the utility benefits of PAC privacy.

Second, if we set $b' \gg b$ to preserve utility (i.e., we rely on the P_S -specific bound in Eq. (7)), the recurrence relation becomes:

$$B_t = B_{t-1} + b + b' \sqrt{2B_{t-1}}. \quad (9)$$

We now show that under Eq. (9), the total mutual information bound scales quadratically in T , i.e., $B_T = \Omega(T^2)$.

Since $b > 0$, we have $B_t \geq B_{t-1} + b' \sqrt{B_{t-1}}$. Taking the square root of both sides and applying the inequality $\sqrt{x+y} \geq \sqrt{x} + \frac{y}{2\sqrt{x}} - \frac{y^2}{8x\sqrt{x}}$ (derived from Taylor expansion):

$$\sqrt{B_t} \geq \sqrt{B_{t-1} + b' \sqrt{B_{t-1}}} \geq \sqrt{B_{t-1}} + \frac{b'}{2} - \frac{b'^2}{8\sqrt{B_{t-1}}}.$$

Since B_t is strictly increasing at t grows, there exists some t' such that $B_t \geq b'^2$ for all $t \geq t'$. Then, the inequality above becomes

$$\sqrt{B_t} \geq \sqrt{B_{t-1}} + \frac{3b'}{8},$$

which is an arithmetic progression for $\sqrt{B_t}$. Therefore, $\sqrt{B_T} = \Omega(b'T)$ and $B_T = \Omega(b'^2 T^2)$. In other words, the overall mutual information bound grows *quadratically* in the horizon T .

Therefore, under Theorem A.1, one must choose between two suboptimal outcomes: one either calibrates excessive noise to satisfy the input-independent MI bound at the cost of utility, or accepts a quadratic composition bound where at the same level of overall privacy guarantee and noise level, much fewer responses can be allowed. In contrast, with Algorithm 1, we achieve linear composition with instance-based noise calibration.

B Deferred Full Proofs

B.1 Proof of Lemma 3.2

PROOF. We proceed by induction on the time step t .

For $t = 0$, the only possible τ_0 is empty and Algorithm 1 sets $P_0 = P_S = P_{S|\tau_0=\emptyset}$.

Assume the property holds for $t-1$. That is, for any realizable transcript τ_{t-1} , given that $\mathcal{T}_{t-1} = \tau_{t-1}$,

$$P_{t-1} = P_{S|\mathcal{T}_{t-1}=\tau_{t-1}}. \quad (10)$$

Now consider time step t , let $\tau_t = (\tau_{t-1}, (m_t, r_t))$ be a realizable transcript at time t . We derive the density of the posterior of S conditioned on $\mathcal{T}_t = \tau_t$ via Bayes' Rule: $\forall s \in \mathcal{S}$,

$$\begin{aligned} P(s | \tau_t) &= P(s | \tau_{t-1}, m_t, r_t) \\ &\propto P(r_t, m_t | s, \tau_{t-1}) \cdot P(s | \tau_{t-1}) \\ &= P(r_t, m_t | s, \tau_{t-1}) \cdot P_{t-1}(s) \quad (\text{cf. Eq. (10)}) \\ &= P(m_t | s, \tau_{t-1}) \cdot P(r_t | m_t, s, \tau_{t-1}) \cdot P_{t-1}(s) \\ &= P(m_t | \tau_{t-1}) \cdot P(r_t | m_t, s, \tau_{t-1}) \cdot P_{t-1}(s) \quad (\text{cf. Eq. (3)}) \\ &\propto P(r_t | m_t, s, \tau_{t-1}) \cdot P_{t-1}(s). \end{aligned}$$

Conditioned on $S = s$, $\mathcal{T}_{t-1} = \tau_{t-1}$, $M_t = m_t$, we have $R_t = m_t(s) + \mathcal{N}(0, \Sigma_t)$ where $\Sigma_t = \Sigma(P_{t-1}, M_t, b_t)$ is known. Hence, we have $P_{R_t|m_t, s, \tau_{t-1}} = \mathcal{N}(m_t(s), \Sigma_t)$ and

$$P(r_t | m_t, s, \tau_{t-1}) \propto \exp\left(-\frac{1}{2}(r_t - m_t(s))^\top \Sigma_t^{-1}(r_t - m_t(s))\right).$$

Substituting back, we have

$$P(s | \tau_t) \propto \exp\left(-\frac{1}{2}(r_t - m_t(s))^\top \Sigma_t^{-1}(r_t - m_t(s))\right) \cdot P_{t-1}(s),$$

which matches exactly Eq. (4) to compute P_t . \square

B.2 Proof of Theorem 3.3

PROOF. Since $I(S; R_1, \dots, R_T) \leq I(S; (R_1, M_1), \dots, (R_T, M_T)) = I(S; \mathcal{T}_T)$, we prove a stronger guarantee $I(S; \mathcal{T}_T) \leq B_T$.

By the chain rule of mutual information, we have

$$\begin{aligned} I(S; \mathcal{T}_T) &= \sum_{t=1}^T I(S; M_t, R_t \mid \mathcal{T}_{t-1}) \\ &= \sum_{t=1}^T I(S; M_t \mid \mathcal{T}_{t-1}) + I(S; R_t \mid M_t, \mathcal{T}_{t-1}) \\ &= \sum_{t=1}^T I(S; R_t \mid M_t, \mathcal{T}_{t-1}). \end{aligned} \quad (\text{cf. Eq. (3)})$$

We analyze its t -th term:

$$\begin{aligned} I(S; R_t \mid M_t, \mathcal{T}_{t-1}) &= \mathbb{E}_{\tau_{t-1}, m_t} [I(S; R_t \mid \tau_{t-1}, m_t)] \\ &= \mathbb{E}_{\tau_{t-1}, m_t} [I(S; m_t(S) + \mathcal{N}(0, \Sigma(P_{t-1}, m_t, b_t) \mid \tau_{t-1}, m_t))] \\ &= \mathbb{E}_{\tau_{t-1}, m_t} [I(S; m_t(S) + \mathcal{N}(0, \Sigma(P_{S \mid \tau_{t-1}}, m_t, b_t) \mid \tau_{t-1}, m_t))] \quad (11) \\ &= \mathbb{E}_{\tau_{t-1}, m_t} [I_{S \sim P_{S \mid \tau_{t-1}, m_t}} (S; m_t(S) + \mathcal{N}(0, \Sigma(P_{S \mid \tau_{t-1}}, m_t, b_t)))] \\ &= \mathbb{E}_{\tau_{t-1}, m_t} [I_{S \sim P_{S \mid \tau_{t-1}}} (S; m_t(S) + \mathcal{N}(0, \Sigma(P_{S \mid \tau_{t-1}}, m_t, b_t)))] \quad (12) \\ &\leq \mathbb{E}_{\tau_{t-1}, m_t} [b_t] = b_t. \quad (13) \end{aligned}$$

We justify the derivations as follows. Eq. (11) holds as Lemma 3.2 guarantees $P_{t-1} = P_{S \mid \tau_{t-1} = \tau_{t-1}}$ when conditioned on $\mathcal{T}_{t-1} = \tau_{t-1}$, and the additional conditioning on M_t in the prior is redundant due to the adversary's conditional independence (cf. Eq. (3)). This independence also implies Eq. (12), as it allows us to drop M_t from the conditioning in the probability measure. Finally, Eq. (13) follows directly from Definition 3.1.

Summing over t recovers the statement. \square

B.3 Proof of Proposition 5.1

PROOF. Under $y \neq \tilde{y}$, the label is altered by noise, and the probability of retaining this mislabelled sample (x, \tilde{y}) is

$$\Pr(\min_{j \neq \tilde{y}} T_j(r) \geq \Phi^{-1}(1 - \alpha)) \leq \Pr(T_{\tilde{y}}(r) \geq \Phi^{-1}(1 - \alpha)).$$

Here, $T_{\tilde{y}}(r)$ is

$$t = \frac{(e_{\tilde{y}} - e_y)^\top \Sigma^{-1} (r - e_y)}{\sqrt{(e_{\tilde{y}} - e_y)^\top \Sigma^{-1} (e_{\tilde{y}} - e_y)}} = \frac{(e_{\tilde{y}} - e_y)^\top \Sigma^{-1}}{\sqrt{(e_{\tilde{y}} - e_y)^\top \Sigma^{-1} (e_{\tilde{y}} - e_y)}} (r - e_y),$$

where $r \sim \mathcal{N}(e_y, \Sigma)$. Therefore, $t \in \mathbb{R}$ is a linear transformation of $(r - e_y) \sim \mathcal{N}(0, \Sigma)$, and hence follows a normal distribution with zero mean, whose variance is:

$$\begin{aligned} &\frac{(e_{\tilde{y}} - e_y)^\top \Sigma^{-1}}{\sqrt{(e_{\tilde{y}} - e_y)^\top \Sigma^{-1} (e_{\tilde{y}} - e_y)}} \Sigma \left(\frac{(e_{\tilde{y}} - e_y)^\top \Sigma^{-1}}{\sqrt{(e_{\tilde{y}} - e_y)^\top \Sigma^{-1} (e_{\tilde{y}} - e_y)}} \right)^\top \\ &= \frac{(e_{\tilde{y}} - e_y)^\top \Sigma^{-1}}{(e_{\tilde{y}} - e_y)^\top \Sigma^{-1} (e_{\tilde{y}} - e_y)} \Sigma (\Sigma^{-1})^\top (e_{\tilde{y}} - e_y) \\ &= \frac{(e_{\tilde{y}} - e_y)^\top \Sigma^{-1} (e_{\tilde{y}} - e_y)}{(e_{\tilde{y}} - e_y)^\top \Sigma^{-1} (e_{\tilde{y}} - e_y)} = 1. \end{aligned}$$

Therefore, $t \sim \mathcal{N}(0, 1)$, and

$$\Pr(\min_{j \neq \tilde{y}} T_j(r) \geq \Phi^{-1}(1 - \alpha)) \leq \Pr(t \geq \Phi^{-1}(1 - \alpha)) = \alpha,$$

which proves the statement. \square

B.4 Proof of Proposition 6.1

PROOF. Let $Y = \mathbb{1}\{u^* \in S\}$ be the true membership status. Due to the balanced construction of P_S , we have $\Pr(Y = 0) = \Pr(Y = 1) = 0.5$. Let $A : \text{supp}(\mathcal{T}_T) \rightarrow \{0, 1\}$ be a membership inference decision rule. Then its accuracy is

$$\begin{aligned} \text{Accuracy} &= \mathbb{E}_y [\mathbb{E}_{\tau_T} [\mathbb{1}\{A(\tau_t) = y\} \mid Y = y]] \\ &= \mathbb{E}_{\tau_T} [\mathbb{E}_y [\mathbb{1}\{A(\tau_t) = y\} \mid \mathcal{T}_T = \tau_T]] \\ &\leq \mathbb{E}_{\tau_T} [\max_{a \in \{0, 1\}} \mathbb{E}_y [\mathbb{1}\{a = y\} \mid \mathcal{T}_T = \tau_T]]. \end{aligned}$$

Therefore, the following decision rule is optimal:

$$\begin{aligned} A(\tau_T) &= \operatorname{argmax}_{a \in \{0, 1\}} \mathbb{E}_y [\mathbb{1}\{a = y\} \mid \mathcal{T}_T = \tau_T] \\ &= \operatorname{argmax}_{a \in \{0, 1\}} (1/2 \cdot \mathbb{1}\{a = 0\} \Pr(Y = 0 \mid \mathcal{T}_T = \tau_T) \\ &\quad + 1/2 \cdot \mathbb{1}\{a = 1\} \Pr(Y = 1 \mid \mathcal{T}_T = \tau_T)). \end{aligned}$$

This is equivalent to $A(\tau_T) = 1$ if and only if

$$\begin{aligned} \Pr(Y = 0 \mid \mathcal{T}_T = \tau_T) &< \Pr(Y = 1 \mid \mathcal{T}_T = \tau_T) \\ \Leftrightarrow \Pr(Y = 1 \mid \mathcal{T}_T = \tau_T) &> 0.5, \end{aligned}$$

where

$$\Pr(Y = 1 \mid \mathcal{T}_T = \tau_T) = \sum_{S \in \mathcal{S}} \mathbb{1}\{u^* \in S\} \cdot P(S \mid \mathcal{T}_T = \tau_T).$$

This recovers the decision rule A^* in the statement. \square

C Implementation Details

Tabular Datasets. For tabular datasets, we use XGBoost [5] due to its strong empirical performance on structured data. Categorical features are handled using XGBoost's built-in automatic feature processing method, which internally applies appropriate encoding without requiring manual preprocessing. Model selection is performed on the secret training set S using five-fold cross validation. We conduct a grid search over key hyperparameters controlling model capacity, learning dynamics, and regularization. Specifically, we vary the maximum tree depth, learning rate, number of boosting iterations, row/column subsampling ratios, minimum child weight, and the regularization parameter y . The final model is trained on S using the hyperparameter configuration that achieves the best average cross-validation performance.

Image Datasets. For CIFAR-10 and CIFAR-100, we train a Wide-ResNet-28-10 [51] model from scratch. All experiments are conducted using standard data preprocessing and augmentation protocols. Images are randomly cropped with padding and horizontally flipped, followed by normalization. We use ImageNet statistics for normalization, which does not introduce privacy leakage. For stronger data augmentation, we additionally employ CutMix [50] and MixUp [52], where one of the two is randomly applied on each batch. The model is trained without dropout. Optimization is performed with stochastic gradient descent, with momentum set to 0.9 and weight decay set at 5×10^{-4} for regularization. The initial learning rate is set to 0.1 and decayed using a multi-step schedule, with learning rate drops to 20% of the previous epoch at 60 and 120 epochs. All models are trained for a total of 200 epochs. Mixed-precision (FP16) training is enabled to improve efficiency.

Table 6: Average test accuracy (%) of PAC-private responses under various per-step mutual information budgets $2^{-32} \leq b \leq 2^{-4}$ across datasets when privatizing the predicted confidence scores vs one-hot vectors.

Modality	Dataset	Non-Private	Output	$b = \infty$	$b = 2^{-4}$	$b = 2^{-8}$	$b = 2^{-12}$	$b = 2^{-16}$	$b = 2^{-20}$	$b = 2^{-24}$	$b = 2^{-28}$	$b = 2^{-32}$
Tabular	Census Income	87.39	Confidence	87.17	87.16	86.59	74.72	65.55	57.57	52.40	50.62	50.16
			One-Hot	87.17	87.15	86.68	85.92	85.86	85.84	85.84	85.84	85.84
Image	Bank Marketing	91.98	Confidence	91.69	91.69	91.26	84.52	77.64	62.44	53.33	50.86	50.19
			One-Hot	91.69	91.67	91.02	90.36	90.28	90.27	90.27	90.27	90.29
Image	CIFAR-10	97.37	Confidence	95.80	95.79	93.80	45.73	35.86	34.04	33.57	33.45	33.41
			One-Hot	95.80	95.71	93.52	88.35	87.90	87.81	87.80	87.80	87.79
Text	CIFAR-100	84.02	Confidence	77.79	77.72	74.36	35.79	32.36	31.76	31.66	31.63	31.61
			One-Hot	77.79	77.69	75.56	58.38	56.34	56.17	56.13	56.10	56.11
Text	IMDb Reviews	87.10	Confidence	85.13	85.12	84.69	71.91	55.07	51.28	50.32	50.09	50.04
			One-Hot	85.13	85.13	84.46	74.26	69.32	69.16	69.09	69.10	69.10
Text	AG News	91.61	Confidence	90.44	90.39	88.86	62.88	45.41	39.99	38.67	38.34	38.29
			One-Hot	90.44	90.35	87.95	80.18	79.42	79.31	79.27	79.25	79.25

Text Datasets. For NLP tasks, we use a compact BERT-Small [11, 41] architecture initialized from scratch for text classification. The model consists of 4 transformer encoder layers with a hidden dimension of 512, 8 attention heads per layer, and an intermediate feed-forward dimension of 2048. Both hidden-state and attention dropout are set to 0.1. The maximum sequence length is 512 tokens. We use a batch size of 64 and train for up to 50 epochs with early stopping enabled, which monitors the accuracy on a reserved 10% of the training set S . Optimization is done with AdamW [24], using a baseline learning rate of 10^{-4} , linear warm-up for the first 500 steps, and weight decay set to 0.01 for regularization. Mixed-precision (FP16) training is enabled to improve efficiency.

Distillation. For our proof of concept for the proposed privacy-preserving distillation protocol, we use CINIC-10 [7] as an auxiliary dataset. In particular, we only use the ImageNet subset of this dataset to avoid data leakage on CIFAR-10. This constitutes of a total of 210,000 examples. When training the distillation model, we use the same model architecture, i.e., Wide-ResNet-28-10, and the same training recipe as we train the models on subsets of CIFAR-10, with the addition of balanced sampling as the privately labeled distillation dataset is not guaranteed to be balanced after filtering.

D Additional Experimental Results

D.1 Effects of Output Stability

Table 6 presents the test accuracy of PAC-private responses when privatizing the predicted confidence scores compared to one-hot vectors. We note that when the per-step mutual information budget b is relatively large, i.e., $b \geq 2^{-8}$, privatizing confidence scores leads to slightly better utility. This is because in this regime, the noise required for privacy is small, and confidence scores provide more information than the one-hot predictions. However, when the per-step MI budget gets smaller, the utility of the PAC-private confidence scores rapidly drops to a much lower level compared to the one-hot predictions. In particular, when $b = 2^{-32}$, for the three binary classification tasks, i.e., Census Income, Bank Marketing, and IMDb Reviews, its accuracy collapses to triviality (around 50%), the same as the random guessing baseline. This is because the confidence scores are much less stable than the one-hot predictions, which leads to excessive amounts of noise required to hide the secret set S when the per-step privacy budget b approaches zero.